MPhil Thesis

Suppression of dephasing and decoherence in open quantum systems

Imperial College London

Department of Physics

David Bartram

December 4, 2010

Abstract

In this thesis, we discuss the possibilities for suppression of decoherence, the loss of purity in an open quantum system, and the related process of dephasing. In the first chapter, we review the literature on the subject of open system dynamics, decoherence and methods of decoherence suppression. In the second chapter, we focus on the specific case of a rotationally hot diatomic molecule as an example of an open quantum system, where molecular vibrational wavepackets are subject to dephasing due to rovibrational coupling. We report analytical and numerical results addressing whether the dephasing rate can be controlled by adjustment of the initial wavepacket phases. It appears that over long timescales, phase-only control is not possible, but for earlier timescales the possibility of phase-only control of dephasing remains. In addition, we point out that the time-dependence of the dephasing process depends significantly upon the degeneracy of the rotational environment states. In the final chapter, we discuss the same system, but apply a qualitatively different method of dephasing suppression based on the nonlinear resonance effect in a driving field. We extend previous work on the topic (Shapiro et al. [1]) by considering the effect of using a train of laser pulses as the driving field, in place of a two-colour continuous-wave laser field. We demonstrate that the pulse train method can be more effective at suppressing dephasing than the two-colour CW case.

Declaration of Originality

All the material in this is my own, and any material from other sources has been appropriately referenced. The majority of Chapter 2 has been drawn from the article *Control of dephasing in rotationally hot molecules* [Phys. Rev. A 81, 043405 (2010)] authored by myself (David Bartram) and Misha Ivanov. This article (in the form accepted for publication) is appended to the thesis.

Contents

1 Introduction and Literature Review **7**

1.1 Dynamics of Open Quantum Systems 7

1.2 Decoherence Theory 9

1.2.1 Master Equations 9

1.2.2 Models of Decoherence 10

1.2.3 A note on "dephasing" as compared to "decoherence" 11

1.2.4 Coherent Control 13

1.3 Suppressing Decoherence 15

1.3.1 Quantum Error Correction 15

1.3.2 Decoherence-Free Subspaces 16

1.3.3 Quantum Bang-Bang Control & Dynamical Decoupling 19

1.3.4 Quantum Zeno Effect 20

2 Control of dephasing in rotationally hot diatomic molecules **23**

2.1 Introduction 23

2.2 Rovibrational dynamics as open system dynamics 23

2.3 Dephasing of molecular vibrational wavepackets due to rotational temperature 25

2.3.1 Characterisation and measurement of wavepacket dephasing 25

2.3.2 Phase-only shaping of the initial wavepacket: analytical estimates and numerical simulations 30

2.3.3 Phase- and amplitude-shaping: squeezed coherent wavepacket and two-state wavepacket 34

2.3.4 Analytical investigation of the signal function $S(t)$ 37

2.3.5 Explanation for the Numerical Results of Section 2.3.3 38

2.3.6 Dependence on the Bath Distribution 39
2.4 Conclusions 40

3 Suppression of rovibrational dephasing by nonlinear resonance 43

3.1 Introduction to nonlinear resonance 43
3.2 The dynamic Stark shift 44
3.3 Nonlinear resonance: diatomic molecule driven by pulse train 46
3.3.1 Control of vibrational dynamics via nonlinear resonance 50
3.3.2 Suppression of dephasing via nonlinear resonance 51

List of Figures

2.1 For the case of flat initial phases ($\theta_v = 0 \forall v$), the J=15 contribution to the signal $\frac{|Q(15,t)|^2}{max[|Q(15,t)|^2]}$ (solid blue line) is compared to the analytic approximation for the peaks $\tilde{Q}(J, NT)$ (dashed green line), where T is the vibrational period and N is an integer. The decay and revival of the single-J contribution seen here is due to the anharmonicity. The figure shows that while the approximation fails to capture the revival dynamics, it approximates the decay quite closely. 31

2.2 For the case of flat initial phases ($\theta_v = 0 \forall v$), the normalised signal function $\frac{S(t)}{max[S(t)]}$ (solid blue line) is compared to the analytic approximation for the peaks $\tilde{S}(NT)$ (dashed green line), where T is the vibrational period and N is an integer. The analytic approximation shows good qualitative agreement with the numerical results, demonstrating that the analytic approximation captures the decay of the signal due to rovibrational coupling. 34

2.3 The same as Fig. 2.2, but with a negative quadratic chirp to the initial phases ($\theta_v = -0.1(v - \bar{v})^2$). Again there is good qualitative agreement - the analytic model shows a similar rise and fall. 35

2.4 The normalised signals as a function of time for three different initial vibrational wavepackets. The first has a Gaussian amplitude profile $|\Psi_g\rangle = \sum_k e^{-k^2/2\sigma^2}|k\rangle$ (solid blue line), the second is a position-squeezed coherent wavepacket at the inner turning point $|\beta_c = \pi, \xi = 0.8\rangle$ (dashed green line) and the third is the wavepacket consisting of two adjacent vibrational states $|\Psi_2\rangle = \frac{1}{\sqrt{2}}(|\bar{v}\rangle + |\bar{v}+1\rangle)$ (dot-dashed red line). Here anharmonicity is zero, so the decay in the signal visibility is purely due to the rovibrational coupling. 36

2.5 The normalised peak visibility $V/\max[V]$ as a function of time (extracted from Figure 2.4) for the three initial wavepackets $|\Psi_g\rangle$ (blue circles),$|\beta_c = \pi, \xi = 0.8\rangle$ (green triangles) and $|\Psi_2\rangle$ (red squares). This shows that for our model, these three different wavepackets show the same dephasing behaviour over time. 36

2.6 The normalised peak visibility $V/\max[V]$ as a function of time for two initial wavepackets, each containing only two vibrational states separated by Δv. Naturally, the case where $\Delta v = 2$ ($|\chi_2\rangle$) (blue squares) beats with twice the frequency of $\Delta v = 1$ ($|\Psi_2\rangle$) (green triangles) . We see that the dephasing behaviour over time is different for the two wavepackets, with the $\Delta v = 2$ wavepacket dephasing more rapidly than the wavepacket with $\Delta v = 1$. This demonstrates a case where *amplitude* modulation of the initial wavepacket has a significant effect on the dephasing dynamics. 39

3.1 Rotor-picture potential energy as a function of the angle ϕ, $V(\phi) = -V_1 \cos(\phi) - V_2 \cos(2\phi)$, for example values of V_1 and V_2. In terms of the driven vibrational motion, ϕ corresponds to the classical phase (conjugated to the action) relative to the stable point of the nonlinear resonance, and the coefficients V_k are determined by the envelope of the driving field and the matrix elements of the molecular polarization [see equations (3.7), (3.8) and (3.18)]. Fig. 3.1(a) shows the case where $V_1 = 1$ and $V_2 = 0$ with a minimum at $\phi = 0$ which can be used to create a non-spreading wavepacket locked in phase to the driving field. In Fig. 3.1(b), $V_1 = 1$ and $V_2 = 0.25$. Note that the addition of the weak V_2 contribution deepens the potential well at $\phi = 0$. In Fig. 3.1(c), $V_1 = 0$ and $V_2 = 1$, giving a double-well potential with minima at $\phi = 0, \pi$. In Fig. 3.1(d), $V_1 = 0.25$ and $V_2 = 1$, and the addition of a weak V_1 results in the two potential wells having different depths. These example cases illustrate the kind of control that may be exerted over the form of the rotor-picture potential, and thus over the effects of the nonlinear resonance on the vibrational wavepacket dynamics. 52

Chapter 1

Introduction and Literature Review

1.1 Dynamics of Open Quantum Systems

An open quantum system consists of a system of interest that is coupled to an environment. While the evolution of the system and the environment together is unitary and governed by the Schrödinger equation, when we trace out the environment and consider the system evolution, it need not be unitary. Non-unitary evolution can include decoherence, in which the purity of quantum states is reduced over time, destroying coherent superpositions and evolving the system towards a mixed state. Another possible consequence of the interaction is dissipation, in which energy is lost from the system to the environment. For a detailed treatment of the dynamics of open systems, see the textbook by Breuer and Petruccione [2]. The theory of open quantum systems is interesting and important from a number of perspectives. Firstly, on a practical level, every quantum system in nature is an open system, and this fact alone necessitates an understanding of open system dynamics. Examples of open systems that have been studied intensively include: an atom in an optical cavity (where the cavity photon modes form the environment) [3], a chemical system in solution [4], a quantum dot embedded in a solid [5], and many more. Secondly, decoherence is seen by many as important to fundamental quantum mechanics, which may relate closely to the "measurement paradox" and the emergence of the classical world from its inherently quantum constituents [6][7]. The connection between decoherence and fundamental interpretations of quantum theory is an area of active research, but lies outside the scope of this review. A third reason for the significance of open system dynamics is its importance to the field of quantum information processing. Perhaps the most significant stumbling block for practical, scalable quantum computing is decoherence. Since quantum information processing relies upon

unitary operations, and quantum memory requires long-lived arbitrary superposition states, the presence of non-unitary dynamics is a significant obstacle. Much work (see for example [8] [9]) focusses on the problem of a hypothetical quantum computer's register of qubits in a noisy background. For an extensive review of quantum information theory, including a discussion of the problems imposed by decoherence, see Galindo 2002 [10].

The following discussion is a basic treatment of the dynamics of such open systems, and follows that in Chapter 3 of the textbook by Breuer and Petruccione [2]. Let us call the Hilbert space of the system $\mathcal{H}_S$ and that of the environment $\mathcal{H}_B$, so that the Hilbert space of the total system is $\mathcal{H}_S \otimes \mathcal{H}_B$. Then the total Hamiltonian is

$$H = H_S \otimes I_B + I_S \otimes H_B + H_I \tag{1.1}$$

Here H_S and H_B are the free Hamiltonians of the system and environment respectively, I_S and I_B are the identity operators in the system and environment subspaces, and H_I is the interaction Hamiltonian. Let us assume that the interaction Hamilton may be written as a tensor product of an operator acting on the system subspace, and one which acts on the environment subspace. This interaction Hamiltonian is here denoted by $H_I = K_S \otimes K_B$. (In general H_I may be expressed as a sum of such tensor products). The density matrix of the total system at time t is $\rho(t) = \rho_S(t) \otimes \rho_B(t)$. The combined system is closed, and will evolve in the usual unitary fashion described by the Schrödinger equation. If we assume that initially the total system is in a known state $\rho(0)$, the solution to the Schrödinger equation is $\rho(t) = U(t,0)\rho(0)U^\dagger(t,0)$ where $U(t,0) = \hat{T}\exp(-itH)$ is the time evolution operator for the total system. Here the time dependence of the Hamiltonian, and the resulting time-ordered form of the time evolution operator, has been omitted for brevity.

If we assume that all observations of interest refer only to the system S, then all observables of interest have the form $A_{S+B} = A \otimes I_B$. This has the following consequence for expectation values:

$$\begin{aligned} \langle A \rangle &= Tr\{A_{S+B}\rho\} = Tr_S\{A\rho_S\} \\ \rho_S &= Tr_B\{\rho\} \end{aligned} \tag{1.2}$$

Here Tr denotes the trace over the full system and Tr_S and Tr_B denote the partial trace over the system

and environment subspace respectively. The quantity of fundamental importance, then, is the "reduced density operator" ρ_S, which evolves as

$$\rho_S(t) = Tr_B\{U(t,0)\rho(0)U^\dagger(t,0)\} \tag{1.3}$$

While the total system must evolve unitarily, the system S need not. As a result, open quantum systems can display dynamics quite different from ordinary coherent Schrödinger evolution, including evolution from pure initial states to mixed states. A decrease in purity $Tr\{\rho_S^2\}$, which results in a decay of coherences in the system density matrix, is referred to as decoherence. In general there may also be dissipation - loss of energy from the system to the environment.

While it is formally valid to arbitrarily partition any Hilbert space into "system" and "environment" subspaces, it is important to note that in order for the usual conclusions of decoherence theory to apply, certain assumptions must be made about the environment. These assumptions and their various consequences are discussed in detail in [2]. For example, an environment is often considered to contain many more accessible states than the system. It is also common to assume that transfer of energy and/or entropy proceeds one-way from the system to the environment. If the environment is a continuum with an infinite number of degrees of freedom, it is referred to as a *reservoir*. A reservoir in thermal equilibrium at some temperature T is referred to as a *bath* or *heat bath*.

The rest of this chapter consists of a review of the literature associated with the field of decoherence, and in particular with techniques for its suppression.

1.2 Decoherence Theory

1.2.1 Master Equations

A master equation (the fundamental equation for the dynamics of an open system) is an an equation for the system density operator $\rho_S(t)$, derived by calculating the dynamics in $\mathcal{H}_S \otimes \mathcal{H}_B$ and then tracing over the environment subspace.

In order to derive the standard Lindblad form [11] of the master equation, we must make certain assumptions. Firstly, we must assume that initially, the system and bath density matrices are uncoupled (as opposed to entangled), ie: $\rho(t=0) = \rho_S(0) \otimes \rho_B(0)$. Secondly, we assume that the system density matrix

retains all the properties of a density matrix throughout its evolution, including "complete positivity". In addition, one makes the Markov approximation, which is to assume that the characteristic timescale over which correlations in the environment decay is much shorter than the characteristic time scale of the system evolution. It is important to note that this assumption, which underlies much of decoherence theory, is not always appropriate for real physical systems, and much recent research has been undertaken into non-Markovian dynamics (see for example [12]).

In any case, when the above assumptions hold, the following Lindblad master equation may be derived:

$$\begin{aligned} \partial_t \rho_S &= \mathcal{L}_S\left[\rho_S\right] + \mathcal{L}_D\left[\rho_S\right] \\ \mathcal{L}_D &= \sum_{i,j} \mathbf{A}_{ij} \mathcal{L}_{F_i,F_j} \\ \mathcal{L}_{F_i,F_j}[\rho_S] &= \left[F_i, \rho_S F_j^\dagger\right] + \left[F_i \rho_S, F_j^\dagger\right] \end{aligned} \tag{1.4}$$

Where $\mathcal{L}_S$ and $\mathcal{L}_D$ are system-space Louville superoperators, ie: maps from the space of operators on the Hilbert space $\mathcal{H}_S$ to itself. $\mathcal{L}_S[\rho_S] = -i\left[H_S, \rho_S\right]$ describes the free, unitary Heisenberg evolution of the system, while $\mathcal{L}_D$ describes the system dynamics induced by the system-environment interaction, including decoherence and dissipation. $\mathbf{A}$ is a time-independent Hermitian coefficient matrix containing various parameters related to the decoherence and dissipation. The F_i's are a set of operators called the decoherence generators or error generators, which characterise the coupling between the system and environment [13]. They are often implicitly determined from the interaction Hamiltonian, when it is written as a sum of tensor products $H_I = \sum_\alpha F_S^\alpha \otimes K_B^\alpha$.

1.2.2 Models of Decoherence

A small number of canonical models serve as the basis for much (but not all) of decoherence theory. They are as follows [2]:

i) "Quantum Brownian motion": A harmonic oscillator coupled to a bath of harmonic oscillators

ii) "Spin-boson model": A two-level system (or spin-$\frac{1}{2}$ particle) coupled to a bath of harmonic oscillators

iii) "Spin-spin model": A two-level system coupled to a bath of two-level systems

Recently, work by Schlosshauer et al. [14] has focussed on the fourth combination of the above elements, namely the "oscillator-spin model" in which a harmonic oscillator is coupled to a bath of two-level systems,

a setup that was previously neglected.

At this stage, it is important to note that true decoherence is an inherently quantum phenomenon resulting from *entanglement* between the (initially separable) system and environment states [7]. An ensemble of quantum systems can also be subject to classical noise, resulting in the loss of phase coherence between different systems in the ensemble. While superficially similar to true decoherence, such pure dephasing is theoretically and observationally distinct. This distinction is the topic of the following subsection.

1.2.3 A note on "dephasing" as compared to "decoherence"

The term "decoherence" is not used consistently throughout the literature. It is important to distinguish between true decoherence, which is a deterministic entanglement of system and environment resulting in phase delocalisation, and pure dephasing, which results (for example) from a classical average over an ensemble of systems, each of which is subject to a different Hamiltonian. This is discussed in Chapter 2 of [7]. There Schlosshauer argues that while there may be formal and physical similarities between the two processes, they are both theoretically and (in principle) observationally distinct. Pure dephasing often results in dynamics that can be reversible, whereas true decoherence can lead to irreversible processes (ie: processes which cannot be reversed by unitary operations on the system subspace alone). Pure dephasing is closely related - often synonymous - with the process known as "inhomogeneous broadening". Take for example, the case of spins observed via NMR. Here spatial inhomogeneities in the magnetic field lead to different precession rates for different spins, and the spins dephase over time. However, application of a π-pulse causes the dephasing process to reverse, leading over time to rephasing and the recreation of the original signal. This is the so-called "spin echo" technique of Hahn [15].

In [7], Schlosshauer also argues that a key distinction between classical noise or pure dephasing and real decoherence is that in the latter case, the system perturbs the environment in addition to being perturbed by it. What follows is a derivation that demonstrates this point, showing that if the environment's dynamics are unchanged by the coupling to the system, the resulting system dynamics take the form of a classical average over different environment-dependent unitary evolutions.

Consider the special case where the environment is initially in an eigenstate $|\chi_n\rangle$ of the environment Hamiltonian and in addition, the environment part of the interaction Hamiltonian, K_B, commutes with H_B. This means that the system-environment interaction does not couple different eigenstates of the free environment Hamiltonian. In this case K_B and H_B share a common eigenbasis:

$$\begin{aligned}
[K_B, H_B] &= 0 \\
H_B|\chi_n\rangle &= E_n|\chi_n\rangle \\
K_B|\chi_n\rangle &= \lambda_n|\chi_n\rangle
\end{aligned} \tag{1.5}$$

The total state of the system at time t may be written as

$$|\Psi(t)\rangle = |\phi(t)\rangle|\chi_n\rangle e^{-iE_n t} \tag{1.6}$$

Substituting this ansatz into the Schrödinger equation gives

$$\begin{aligned}
i\partial_t|\Psi(t)\rangle &= \left(H_S \otimes I_B + I_S \otimes H_B + K_S \otimes K_B\right)|\phi(t)\rangle|\chi_n\rangle e^{-iE_n t} \\
&= \left(\left[H_S + E_n I_S + \lambda_n K_S\right] \otimes I_B\right)|\phi(t)\rangle|\chi_n\rangle e^{-iE_n t}
\end{aligned} \tag{1.7}$$

Taking the time derivative of equation (1.6) directly gives

$$i\partial_t|\Psi(t)\rangle = e^{-iE_n t}\left(i\left[\partial_t|\phi(t)\rangle\right]|\chi_n\rangle + E_n|\phi(t)\rangle|\chi_n\rangle\right) \tag{1.8}$$

Substituting this result into equation (1.7) and premultiplying by $e^{+iE_n t}\langle\chi_n|$ shows that the ansatz is valid if the following equation governs the evolution of the system state:

$$i\partial_t|\phi(t)\rangle = \left(H_S + \lambda_n K_S\right)|\phi(t)\rangle \tag{1.9}$$

Which is to say in this case (where the environment state is the nth eigenstate of its free Hamiltonian and $[K_B, H_B] = 0$), the system evolves *unitarily* under an n-dependent Hamiltonian $\tilde{H}_S^n = H_S + \lambda_n K_S$. The environment state remains in the energy eigenstate $|\chi_n\rangle$, and simply accrues a time-dependent phase factor $e^{-iE_n t}$.

We may also consider the slightly more general case where the initial state of the environment is in a mixed state (incoherent superposition) of energy eigenstates $\rho_B(0) = \sum_n p_n|\chi_n\rangle\langle\chi_n|$, where the p_n's are

non-negative real numbers satisfying $\sum_n p_n = 1$. An example of such a state is the thermal equilibrium state where the p_n's are just the Boltzmann occupation probabilities $P(E_n)$.In such a case, the consequence of $[K_B, H_B] = 0$ is that we can express the evolution of the system density matrix as

$$\rho_S(t) = \sum_n p_n \tilde{U}_S^n(t,0)\rho_S(0)\tilde{U}_S^{n\dagger}(t,0) \tag{1.10}$$

Here $\tilde{U}_S^n(t,0) = \exp(-it\tilde{H}_S^n)$. So for this case, the result of the system-environment interaction is the same as a classical (incoherent) average over the bath states. The environment affects the system, in that the system Hamiltonian is n-dependent, but the environment evolves as if the system were not present. Different system energy levels are coupled via the environment states, but the environment states remain uncoupled.

This result is only valid if K_B commutes with H_B. Truly irreversible dynamics can occur when the system-environment interaction causes non-trivial dynamics of both the system and the environment.

1.2.4 Coherent Control

Coherent control is a method of control over quantum systems in which quantum interference effects are used to alter observable properties of a quantum system [16]. Coherent control of chemical processes using laser fields was first proposed by Brumer and Shapiro in the late 1980s [17], and significant experimental progress in this field has been made since the early 1990s [18]. Coherent control over photodissociation processes has been demonstrated (see for example [19]). By arranging interference between multiple indistinguishable optical excitation routes, control over the yields of different photodissociation products can be achieved with weak control fields. Such weak-field control is often straightforward to describe theoretically using perturbation theory (see Chapter 3 of the textbook by Brumer and Shapiro [16]). In cases where one can calculate the effect of the field on the system to sufficient accuracy, one may compute the control field required to optimise a particular parameter (for example, the yield of a particular product). Calculation of such optimal control fields may be performed using Optimal Control Theory, an extension of the calculus of variations (see Chapter 4 of [16]). In general, numerically calculating the optimal control field and then subsequently implementing it in the laboratory is termed "open-loop control".

Open-loop control will fail in cases where the dynamics of the system under the effect of the control field are too complex to approach computationally - such as for polyatomic molecules, or when the laser field is too strong for perturbation theory to apply. In such cases one may turn to the "closed-loop control" proposed

by Judson and Rabitz in 1992 [20]. The concept of "closed-loop control" can be described as allowing the molecular system itself solve it's own Schrödinger equation. Here one defines a fitness parameter for optimisation which can be rapidly measured in the laboratory. Then one repeatedly applies different pulse shapes to the molecular sample, and measure the resulting fitness parameter for each pulse shape. One alters the control pulse shape according to some 'learning algorithm' which is designed to seek out the global optimum in the control parameter space. Genetic algorithms are often used, whereby an initially random population of control pulses is tested, from which only the best "survive" to the next "generation". By introducing random mutation of the control parameters and a steady influx of new, randomly created control pulses, an algorithm may be created which is effective in escaping any local optima [20]. The experimental results gained using closed-loop coherent control are numerous - one example is the strong-field control of chemical dissociation and reaction channels in various organic molecules reported by Levis et al. [21]. Another is the use of a holographic reconstruction technique and a closed-loop iteration to tailor the wavefunction of an atomic Rydberg electron [22].

At this stage it is worth noting that the search space for optimisation is often extremely extensive, and finding the global optimum may be difficult even for a learning algorithm. As a result, in current research there is a role for both open- and closed-loop quantum control. Coherent control in open systems (see Chapter 5 of [16]) is a subject of considerable research - for example [23] addresses the optimisation landscape for open systems, while [24] applies optimal control theory to the design of quantum computational gates for solid-state quantum dot qubits. Shuang and Rabitz [25] even show that under some conditions it is possible for decoherence to *assist* the control field in achieving the objective. When addressing a particular goal in a particular quantum system, then, one should consider whether to try to suppress decoherence, or co-operate with it. On a similar note, Plenio and Huelga [26] argue that dephasing noise can be beneficial, rather than detrimental, to certain essential transport processes in light-harvesting biomolecules - nature may already be taking advantage of the inevitability of environmental interactions. Another case where an open system's non-unitary dynamics can be advantageous is the laser cooling of the so-called 3-level Λ system. As discussed by, for example, Sklarz et al. [27], the cooling of a system requires a reduction in its entropy - so that we are in fact considering non-unitary dynamics that *increase* the purity of the system state. The laser itself, of course, acts unitarily on the *system* Hilbert space, and not on the *environment* (the electromagnetic vacuum fluctuations) and so cannot itself achieve a change in entropy or purity. In the "laser cooling" of a Λ system, the laser steers the system into a configuration where the dissipative dynamics induced by the environment actually cool the system. Such processes are the exception rather than the rule

- most commonly, decoherent and dissipative dynamics form an obstacle to successful coherent control of a system. In Section 2.3.1, we discuss whether the case of phase adjustment of a vibrational wavepacket, in the hope of creating a wavepacket resistant to rovibrational dephasing, can be correctly classified as coherent control.

1.3 Suppressing Decoherence

1.3.1 Quantum Error Correction

If we neither suppress decoherence processes using an external control, nor encode our information in a decoherence-free subspace, we can still think of combating decoherence by *reversing* its effects. This would require a scheme that permitted us to determine which errors our decoherence have introduced, and correct them with an external control. The idea is based on analogy with error correcting codes in classical information theory, which operate on a similar principle. However, it was not immediately obvious that classical error correction could be generalised to quantum information, for a number of reasons [28]. For example, it was not immediately clear how to adapt these methods to correct the *phase* errors that may occur in quantum systems. Additionally, in order to correct an error we must be able to measure it, and there is a danger that the measurement will destroy the quantum information we are hoping to protect. Finally, to protect against errors we must encode information in a redundant manner, but the "No-Cloning Theorem" [29] states that we cannot copy a quantum state, so the possibility of redundant encoding was called into question.

These difficulties can, in fact, be overcome. Quantum error correction (QEC) was first proposed by Shor in 1995 [30], with other seminal work being done by Steane [31] and others. The link between classical error-correcting codes and QEC is clearly demonstrated by Steane's code, which is directly based on the classical "[7,4,3] Hamming code", and enables the storage of one qubit using a total of seven qubits. Calderbank and Shor [32] showed in 1996 that "good" QEC codes existed, i.e. ones capable of correcting numerous errors. The idea behind QEC is to encode k qubits of quantum information using a system comprising $m > k$ qubits, in such a way that we will be able to perform a computation that allows us to measure *only* the errors that have occurred, without measuring (and thus disturbing) the encoded information itself. If this can be achieved, then quantum computational operations can be employed to undo the errors, restoring the initial quantum information without disrupting its coherence by direct measurement.

One drawback of QEC codes is that they are formulated for Markovian decoherence processes. Real

physical systems can display non-Markovian dynamics (even if there is a timescale over which the Markov approximation is effective), which could severely reduce the effectiveness of QEC techniques. Fischer and Loss [33] argue that decoherence is system-specific rather than generic, and that decoherence suppression is best achieved by understanding the details of the specific system one is examining. This argument also applies to other techniques like decoherence-free subspaces (Section 1.3.2) and dynamical decoupling (Section 1.3.3), in that abstract models of "generic" decoherence processes may fail to capture key elements of the process in a specific physical system. It is also worth noting that QEC schemes can prove insufficient if the rate of decoherence is too fast. As a result, it is reasonable to suggest that in practice, QEC should be combined with other methods that actively suppress the rate of decoherence. In the case of ro-vibrational dephasing of a vibrational wavepacket in a diatomic molecule, the nonlinear resonance method discussed in Chapter 3 is an example of a method that actively suppresses the dephasing rate, and it could potentially be used in conjunction with a QEC scheme to protect vibrational qubits.

1.3.2 Decoherence-Free Subspaces

Rather than attempting to suppress decoherence via some external interaction, under certain conditions it may be possible to avoid it altogether. For some Hamiltonians, there exist subspaces of the system Hilbert space which evolve unitarily. Lidar et al. coined the term "decoherence-free subspaces" or "DFS" to refer to these, and they have been the subject of much theoretical work (for a comprehensive review from 2003 see Lidar and Whaley [34]).

Consider an open system S coupled to an environment B with Hilbert space $\mathcal{H}_S \otimes \mathcal{H}_B$ and Hamiltonian given by equation (2.1). The interaction Hamiltonian can be written as a sum of tensor products of system and environment operators $H_I = \sum_\alpha F_\alpha^S \otimes K_\alpha^B$ [2] - the operators F_α are often called the "error generators". A decoherence-free subspace $\tilde{\mathcal{H}}_S$ can be defined as a subspace of the system Hilbert space in which the time evolution is unitary. This is true if and only if three conditions are satisfied [35][13]:

i) All of the basis states $\{|\tilde{\imath}\rangle\}$ of $\tilde{\mathcal{H}}_S$ must be degenerate eigenstates of all the error generators:

$$F_\alpha|\tilde{\imath}\rangle = c^\alpha|\tilde{\imath}\rangle \qquad \forall\tilde{\imath},\alpha \tag{1.11}$$

Here c^α is a complex number that depends only on α, the index over error generators. So all the basis states $\{|\tilde{\imath}\rangle\}$ of the DFS must share the same eigenvalue c^α of any given error generator F_α.

ii) The system is initially decoupled from the environment:

$$\rho(t=0) = \rho_S(0) \otimes \rho_B(0) \tag{1.12}$$

iii) The free system Hamiltonian does not mix states within the subspace with states outside it:

$$\begin{aligned} \langle j|H_S|\tilde{\imath}\rangle = 0 \\ \forall \tilde{\imath}, j \end{aligned} \tag{1.13}$$

Here the index $\tilde{\imath}$ runs over states in the subspace and j runs over states outside the subspace.

The existence of such subspaces arises from dynamical symmetries, and so determining whether they exist (and finding them if they do) requires a group theoretical treatment. Indeed, the question reduces to a standard problem in the representation theory of Lie algebras [13].

As a very simple example of a decoherence-free subspace, consider the case where the system is formed by two identical qubits (two-level systems), denoted by a and b. We assume that the effect of the environment can be modelled as a collective bit-flip - every so often both qubits are "flipped", so that $|1\rangle \to |0\rangle$ and $|0\rangle \to |1\rangle$. The error generator for this process is $F_1 = \sigma_a^x \otimes \sigma_b^x$, where σ^x is the usual Pauli operator.

It is easy to see that the states $|\Psi\rangle_{ab} = \frac{1}{\sqrt{2}}(|0\rangle_a|0\rangle_b + |1\rangle_a|1\rangle_b)$ and $|\Phi\rangle_{ab} = \frac{1}{\sqrt{2}}(|0\rangle_a|1\rangle_b + |1\rangle_a|0\rangle_b)$ are invariant under F^1. Since $|\Psi\rangle_{ab}$ and $|\Phi\rangle_{ab}$ are orthogonal, we can use them as basis states to encode a single qubit of quantum information, which will be completely resistant to the collective bit-flip noise. Thus, within the 4-dimensional Hilbert space $\mathcal{H}_{ab}$ there is a 2-dimensional DFS spanned by $\{|\Psi\rangle_{ab}, |\Phi\rangle_{ab}\}$.

The remaining subspace, spanned by $|\Theta\rangle_{ab} = \frac{1}{\sqrt{2}}(|0\rangle_a|1\rangle_b - |1\rangle_a|0\rangle_b)$ and $|\Lambda\rangle_{ab} = \frac{1}{\sqrt{2}}(|0\rangle_a|1\rangle_b + |1\rangle_a|0\rangle_b)$ is also decoherence-free by equation (1.11), since both basis states are eigenstates of F_1 with eigenvalue -1.

Note that the details of the external interaction are significant, since they determine the dynamical symmetries. In the above example the collective nature of the spin-flip operation is highly significant - if the qubits are allowed to decohere independently, the dynamical symmetry is altered. Consider the case where, in addition to the possibility of a collective bit-flip, there is a chance for qubit a or qubit b to flip, leaving the other qubit unchanged. Then we must include a further two error generators $F_2 = \sigma_a^x \otimes I_b$ and $F_3 = I_a \otimes \sigma_b^x$, where I is the identity operator.

Under such operations $|\Psi\rangle_{ab} \to |\Phi\rangle_{ab}$ and $|\Phi\rangle_{ab} \to |\Psi\rangle_{ab}$. Both F_2 and F_3 are equivalent to the bit-flip

operator σ_x in the $\{|\Psi\rangle_{ab}, |\Phi\rangle_{ab}\}$ basis. The only state in the $\{|\Psi\rangle_{ab}, |\Phi\rangle_{ab}\}$ eigenspace of F_1 that is *also* invariant under F_2 and F_3 is $|\Xi\rangle = \frac{1}{\sqrt{2}}(|\Psi\rangle_{ab} + |\Phi\rangle_{ab})$. As a result, the only decoherence-free subspace is one-dimensional, and thus not large enough to encode even a single qubit of information.

Similarly, the F_1 eigenspace spanned by $\{|\Theta\rangle_{ab}, |\Lambda\rangle_{ab}\}$ provides only a one-dimensional DFS under F_2 and F_3 spanned by $|\Gamma\rangle = \frac{1}{\sqrt{2}}(|\Theta\rangle_{ab} + |\Lambda\rangle_{ab})$. The two decoherence-free states $|\Xi\rangle$ and $|\Gamma\rangle$ cannot be used as a basis for a two-dimensional DFS, since they belong to different eigenspaces of F_1 and F_3. Thus, the error generators will introduce phase flips within any superposition of these two states, if one were to use such a superposition to store a qubit.

There exists a generalisation of the decoherence-free subspace, namely the decoherence-free sub*system* [34]. The basic concept here, is rather than considering subspaces of $\mathcal{H}_S$, one instead considers subsystems S_1 and S_2 such that $\mathcal{H}_S = \mathcal{H}_{S_1} \otimes \mathcal{H}_{S_2}$. A decoherence-free subsystem is then a subsystem S_1 whose dynamics are purely unitary. Then information can be encoded in this subsystem, so that the initial system density operator is $\rho_S(0) = \rho_{S_1}(0) \otimes \rho_{S_2}(0)$, such that ρ_{S_1} is completely protected from decoherence, while ρ_{S_2} is subject to decoherence. The decoherence-free subspace is a special case of the decoherence-free subsystem.

It is important to note that decoherence-free subspaces do not provide a general recipe for avoiding every kind of decoherence, since the requirements for them to exist are stringent, and the underlying assumptions of the theory may be too unrealistic. For complex multiparticle systems, identification and exploitation of DFSs could be extremely difficult, if they exist at all. In cases where there are multiple mechanisms of decoherence, or where the Hamiltonian is not completely known, determining any decoherence-free subspaces or subsystems could be difficult or impossible.

Despite these drawbacks, Lidar and Whaley [34] argue that decoherence-free subspaces provide a powerful tool for protecting against decoherence. Decoherence-free subspaces, where they exist, are stable to first order against symmetry-breaking perturbations [13]. Lidar and Whaley propose that, where the necessary dynamical symmetries are present, decoherence-free subspaces should be used as a first resort before turning to higher-level methods of protection including quantum error-correcting codes (see Section 1.3.1 of this report) and dynamical decoupling via external fields (Section 1.3.3). The benefits of decoherence-free subspaces have been verified experimentally - one example is the demonstration of a two-qubit DFS protecting the state of two photons under engineered collective dephasing [36], another is the use of the same two-qubit DFS to reduce ambient decoherence in ion-trap experiments [37].

1.3.3 Quantum Bang-Bang Control & Dynamical Decoupling

Quantum bang-bang control (named in analogy to its classical counterpart), is a method of active decoherence suppression which uses external control fields which interact with the system dynamics on a time-scale shorter than the characteristic memory time of the environment. It is closely related to decoherence-free subspaces (see Section 1.3.2), in that we may think of the bang-bang control field as symmetrising the system-bath interaction, thus *creating* a decoherence-free subspace [34][38].

The following is a simple example of quantum bang-bang control based on Byrd and Lidar [39]. Consider an open system with the usual Hamiltonian (1.1). The control pulse, which acts only on the system dynamics, has Hamiltonian $H^c = H_S^c \otimes I_B$ and (short) duration Δt. We assume that the control pulse can be chosen such that its time-evolution operator $U_c \simeq e^{-iH^c\Delta t}$ has the following properties:

$$\begin{aligned} [U_c, H_S] &= 0 \\ \{U_c, H_I\} &= 0 \end{aligned} \tag{1.14}$$

ie: U_c commutes with the system Hamiltonian, but anticommutes with the interaction Hamiltonian. We assume that we can also apply the inverse control pulse, ie: a pulse with Hamiltonian $-H_c$ and duration Δt, yielding the time evolution operator $U_c^\dagger$. If, at time t_0, we apply U_c followed by $U_c^\dagger$, the total time evolution operator is given by the following equation (if Δt is shorter than the characteristic timescale of the dynamics - this works perfectly in the limit of continuous pulsing, ie: $\Delta t \to 0$):

$$\begin{aligned} U(2\Delta t, t_0) &= U_c e^{-iH\Delta t} U_c^\dagger e^{-iH\Delta t} \\ &= e^{-i\left(U_c H U_c^\dagger\right)\Delta t} e^{-iH\Delta t} \\ &= e^{-i\Delta t(H_S\otimes I_B + I_S\otimes H_B - H_I)} e^{-i\Delta t(H_S\otimes I_B + I_S\otimes H_B + H_I)} \\ &= e^{-i2\Delta t(H_S\otimes I_B + I_S\otimes H_B)} \end{aligned} \tag{1.15}$$

From this simple example it is easy to see how, under certain assumptions, frequent application of short pulses can average out, or symmetrise, the system-bath interaction. The result is that the system evolves in a completely unitary, decoherence-free fashion. A key goal of quantum bang-bang control theory is to establish how effective such techniques are under more realistic constraints - obviously the continuous-pulse limit is not physically realisable. While the ideal case is unattainable, theoretical research (see for example [40][41]) has

shown that bang-bang techniques can provide a substantial reduction in decoherence and dissipation for two-level systems coupled to baths, as long as the control pulse duration Δt is much less than the characteristic memory time of the bath.

Dynamical decoupling [42] is a powerful generalisation of quantum bang-bang control theory, which determines how and whether it is possible, given a set of realisable control operations, to dynamically create a decoherence-free subspace in the system Hilbert space. Bang-bang methods are those which dynamically ensure that the whole system Hilbert space is decoherence-free, and thus constitute a special case of dynamical decoupling. Dynamical decoupling is a powerful formalism enabling open-loop suppression of decoherence, with a wider scope of applicability than the original bang-bang proposals.

There are some practical drawbacks of bang-bang control and dynamical decoupling. One is that the creation of sufficiently short, intense and frequent interaction pulses may be extremely challenging. Another is that such intense driving fields will tend to induce nonlinear effects on the system, severely altering its dynamics.

1.3.4 Quantum Zeno Effect

The Quantum Zeno Effect (QZE) is the inhibition of decay of an unstable quantum system by continuous (or sufficiently frequent) projective measurement. It is a feature of quantum mechanics that has been known for some decades [43]. Note that the QZE applies to *induced* decay as well as to spontaneous decay. In 1990 Itano et al. [44] observed the effect experimentally, using laser-cooled Beryllium-9 ions in a Penning trap. The decay in question was a radio-frequency-induced transition between hyperfine levels of the ion's ground state, and the frequent measurement was provided by a sequence of short light pulses. Their results closely matched theoretical predictions. This applicability of the QZE to induced decay makes clear the conceptual connection to the theory of open systems, since the Itano experiment could be said to demonstrate protection of a system of interest (the ion's electronic degree of freedom) from an external environment (the applied RF field). Of course, in this example the connection is not a practical one, since the applied RF field does not have the usual properties of a reservoir or thermal bath.

The QZE was once thought to be a universal property of unstable quantum systems, but Kofman and Kurizki [45] have shown that for a class of quantum systems (including spontaneous emission from a two-level system in a vacuum), it is inherently impossible. Indeed, the opposite effect is more likely to occur, whereby frequent measurements of the system *enhance* the decay process. This is dubbed the quantum anti-Zeno effect (QAZE), or inverse Zeno effect. The quantum anti-Zeno effect also occurs for processes which admit

the ordinary QZE, if the repeated measurements are insufficiently frequent.

The QZE, used as a tool for suppression of decoherence, is closely related to bang-bang decoupling techniques. Facchi et al. [46] show that the decoherence-free subspaces created by dynamical decoupling can be seen as a special case of the Zeno subspaces created by frequent interaction with an external environment. This extends the techniques provided by bang-bang decoupling, allowing suppression of decoherence using external fields with no particular symmetry properties with respect to the system (in contrast with the requirements of equation (1.14) in Section 1.3.3 above). Thanks to the quantum anti-Zeno effect, drawing the connection between dynamical decoupling and the QZE also illustrates the possibility that attempts at bang-bang decoupling could in fact *worsen* the effects of the system-environment interaction.

Chapter 2

Control of dephasing in rotationally hot diatomic molecules

2.1 Introduction

In this chapter, we consider a rotationally hot diatomic molecule as an example of an open quantum system, where molecular vibrational wavepackets are subject to dephasing due to rovibrational coupling. We report analytical and numerical results addressing whether the dephasing rate can be controlled by adjustment of the initial wavepacket phases. It appears that over long timescales, phase-only control is not possible, but for earlier timescales the possibility of phase-only control of dephasing remains. In addition, we point out that the time-dependence of the dephasing process depends significantly upon the degeneracy of the rotational environment states.

2.2 Rovibrational dynamics as open system dynamics

Previous sections have addressed methods for protecting a general system of qubits from decoherence. Now we focus on the case where the system of interest is a molecule. This is by no means unrelated to the discussions of previous sections. Molecular states can be used to encode quantum information, for example by selecting a particular vibrational mode, and designating a particular excitation of that mode to be the qubit state $|1\rangle$ and another, the qubit state $|0\rangle$. In such a scheme, a single molecule can store multiple independent vibrational qubits, one for each vibrational normal mode. Then quantum computational operations can

be performed using laser light [47]. There is a close connection between vibrational and rovibrational molecular quantum computing and the theory of coherent control, in that the specific laser pulse required to perform a particular quantum computation must be determined by open- or closed-loop optimisation. This conceptual connection between molecular quantum dynamics and quantum information theory runs both ways. Shapiro et al. [48] propose an approach to coherent control of vibrational wavepackets that uses concepts from quantum information processing, allowing the formulation of open-loop control procedures built from elementary quantum-logical operations. The same approach is taken to rotational wavepackets by Lee et al. [49].

When a molecule's dynamics are affected by an interaction with an external environment - for example with a solvent, with a surface or with collision partners in the gas phase - the usual Lindblad formulation for open system dynamics may be applied [50]. Thus a molecule in an environment is a useful example of an open quantum system. One example of a decoherence suppression technique for molecules is the proposal by Katz et al. [51]. Their scheme involves using the time-dependent state of a molecule isolated from a particular decohering environment as a "target" for controlling the dynamics of a molecule which is coupled to the environment. The control field is optimised to maximise the overlap between the open molecular system and the isolated system, thus extending the decoherence lifetime of the open system.

One way to consider molecular dynamics as a model of a system subject to decoherence is to define the "system" as the vibrational degree of freedom of the molecule, and the"environment" as the rotational degree of freedom [52] [53]. For potassium and sodium dimers, it is practically straightforward to achieve vapour temperatures at which 100 rotational levels, but very few vibrational levels, are thermally populated - making the rotational degree of freedom a good model for a thermal bath. These degrees of freedom are coupled via the moment of inertia, and as a result the ro-vibrational coupling can be seen as a mechanism for "environment"-induced decoherence of a vibrational wavepacket. Two things are important to note - that such a wavepacket undergoes only pure *dephasing*, and not dissipation or true decoherence. Indeed, if the molecular potential is harmonic, then the coherence will undergo periodic collapse and revivals [54]. The concept of re-phasing and revival is absent from standard treatments of decoherence, since it is generally impossible in cases of true decoherence, where the system and environment become entangled over time.

So while this model certainly does not capture all of the features of real environment-induced decoherence, it provides a well-understood system-environment model on which to test methods for decoherence suppression. While there exist no decoherence-free subspaces for this system, in [53] and [52] phase-space considerations based on the Wigner function are used to argue that there are initial wavepackets which are

more *resistant* to the dephasing process, and that closed-loop optimal control could be used to find those wavepackets. This idea was experimentally applied by the Walmsley group - their results are described in a Science paper [55] which described the procedure as "coherent control of decoherence". This description overstates the matter somewhat, since the pure dephasing caused by the rovibrational interaction does not represent true decoherence, and the use of closed-loop optimisation to find dephasing-resistant wavepackets does not constitute control over the dephasing *process*.

At temperatures around 400°C (typical for production of alkali dimers from an oven source), ~ 100 rotational states J will be populated thermally. Note that the rotational state J is $(2J+1)$-fold degenerate. Since the vibrational frequency is dependent on rotational quantum number J thanks to centrifugal distortion, vibrational wavepackets moving on different (J-dependent) potential energy surfaces will dephase over time. We investigate the possibility of controlling this rotationally-induced dephasing process by shaping the initial vibrational wavepacket. The *Science* article by Branderhorst et al. [55] suggests that *phase-only* shaping of the initial wavepacket can have an effect on the dephasing rate. Our work addresses the effectiveness of such phase-only shaping in this particular system.

This chapter contains analytical and numerical results. Numerical simulations show no readily apparent effect of phase-only shaping, except by interaction between the quadratic chirp of the vibrational phases and the anharmonicity. This is just an example of the well-known wavepacket focussing [56] in an anharmonic potential, and does not relate to the thermal dephasing dynamics. In order to understand the numerical results, analytical calculations were performed, including a calculation for zero anharmonicity (the case discussed in [55]). These calculations show that over long timescales, phase-only shaping of the initial wavepacket has no effect on the dephasing. However, at intermediate timescales, the possibility of controlling the dephasing rate remains.

2.3 Dephasing of molecular vibrational wavepackets due to rotational temperature

2.3.1 Characterisation and measurement of wavepacket dephasing

Before discussing the details of wavepacket dynamics in a rotationally hot diatomic molecule, it is important to stress the difference between rotationally-induced dephasing and decoherence associated with entanglement between a system and its environment. This distinction is discussed, for example, in Chapter 2 of [7] and Chapter 3 of [57]. In [7] it is argued that a key distinction between classical noise or pure dephasing

and real decoherence is that in the latter case, the system perturbs the environment in addition to being perturbed by it.

In the standard treatment of an open system [2], we call the Hilbert space of the system $\mathcal{H}_S$ and that of the environment $\mathcal{H}_B$, so that the Hilbert space of the total system is $\mathcal{H}_S \otimes \mathcal{H}_B$. Then the total Hamiltonian is

$$H = H_S \otimes I_B + I_S \otimes H_B + H_I \tag{2.1}$$

Here H_S and H_B are the free Hamiltonians of the system and environment respectively, I_S and I_B are the identity operators in the system and environment subspaces, and H_I is the interaction Hamiltonian.

We now focus on the rovibrational motion of a diatomic molecule. Within the Born-Oppenheimer approximation, assuming the molecule is in a given electronic state $|i\rangle$, it is possible [53] to re-write the rovibrational Hamiltonian for the total system in the following form.

$$\begin{aligned} H &= \frac{\hat{p}^2}{2\mu} + U_i(\hat{R}) + \frac{\hat{J}^2}{2\mu\hat{R}^2} \\ &= \left(\frac{\hat{p}^2}{2\mu} + U_i(\hat{R})\right) \otimes I_r + I_v \otimes \frac{1}{2\mu R_{eq}^2}\hat{J}^2 + \left(\frac{1}{2\mu\hat{R}^2} - \frac{1}{2\mu R_{eq}^2}\right) \otimes \hat{J}^2 \end{aligned} \tag{2.2}$$

Here $\hat{R}$ and $\hat{p}$ are the internuclear co-ordinate and momentum operators respectively, R_{eq} is the equilibrium internuclear distance, μ is the reduced mass, $U_i(R)$ is the molecular potential energy surface, I_r and I_v are the identity operators on the rotational and vibrational subspaces respectively, and $\hat{J}^2$ is the angular momentum operator (in units of $\hbar^2$). In the above form, the rovibrational Hamiltonian resembles the open system Hamiltonian (2.1), with $H_S = \frac{\hat{p}^2}{2\mu} + U_i(\hat{R})$, $H_B = \frac{1}{2\mu R_{eq}^2}\hat{J}^2$ and $H_I = \left(\frac{1}{2\mu\hat{R}^2} - \frac{1}{2\mu R_{eq}^2}\right) \otimes \hat{J}^2$.

Note that in this case $[H_I, H_B] = 0$, so the system-environment interaction does not affect the environment states, i.e.: the rotational J-states. In this case, if the total system starts in a state $|\Psi_v(R)\rangle|J\rangle$, it evolves into $|\Psi_{v,J}(R,t)\rangle|J\rangle$, developing no entanglement. Thus, averaging over the thermal distribution in a rotational ensemble results in pure dephasing. This is to be expected, since the vibrational and rotational parts of the rovibrational wavefunction are always separable.

If the diatomic molecule is modelled as a Morse oscillator, the standard approximation for the energy of the state with vibrational quantum number v and rotational quantum number J is

$$E(v,J) = \omega_e \left(v+\frac{1}{2}\right) - \omega_e x_e \left(v+\frac{1}{2}\right)^2 + \left[B_e - \alpha_e \left(v+\frac{1}{2}\right)\right] J(J+1) - D_e J^2 (J+1)^2 \qquad (2.3)$$

Here ω_e, $\omega_e x_e$,B_e and D_e are the usual spectroscopic constants [58]. If the rotations are confined to a plane, we instead have J^2 wherever $J(J+1)$ appears in (2.3). Since $\langle J \rangle \approx 100 \gg 1$, this difference is negligible.

Equation (2.3) for $E(v,J)$ can be rewritten in the following form by introducing the J-dependent vibrational frequency $\omega_J = \omega_e - \alpha_e J(J+1)$:

$$E(v,J) = \omega_J \left(v+\frac{1}{2}\right) - \omega_e x_e \left(v+\frac{1}{2}\right)^2 + B_e J(J+1) - D_e J^2 (J+1)^2 \qquad (2.4)$$

If we have, for a molecule with a given J, a wavepacket $|\Psi_J(t)\rangle$ over the vibrational states $|vJ\rangle$ (which are J-dependent thanks to the centrifugal distortion), its time evolution is

$$|\Psi_J(t)\rangle = \sum_v a_{vJ} e^{-iE(v,J)t} |vJ\rangle \qquad (2.5)$$

Here a_{vJ} are the wavepacket amplitudes. The rovibrational coupling term in $\omega_J = \omega_e - \alpha_e J^2$ will cause wavepackets for different J-values to dephase with each other over time [54]. This dephasing process is not irreversible; there will be revivals of the phase coherence of the ensemble. In general, however, these revivals will not coincide with the revivals due to the anharmonicity $\omega_e x_e$, and from an observational standpoint the process looks like an irreversible dephasing.

Now we focus on the case of vibrational wavepackets created by one-photon excitation due to a laser pulse, as in the theoretical and experimental work described in references [53] and [55]. We assume that the spectral amplitudes of the pulse have their *phases* shaped at the experimenter's wish, but their *magnitudes* are unaffected by the pulse shaper. In the experiment [55] the molecules under consideration are potassium dimers at 400°C. At this temperature all molecules in the ensemble are in the electronic ground state. For simplicity, we assume that only the ground vibrational state is populated - in fact $\langle v \rangle \approx 1$ at this temperature, but the standard deviation of the thermal distribution $\Delta v_T \approx 3$, so full accuracy would require consideration of the first few vibrational levels. This assumption does not affect our conclusions since the effect of thermal occupation of different vibrational states is similar to that of rotational states. The rotational states are

incoherently populated at temperature T, ie: the rotational density matrix is diagonal with populations $P(J) = Z^{-1}(2J+1)\exp\left\{\frac{-B_e J^2}{kT}\right\}$ where Z is the partition function. Here the $2J+1$ factor appears in the 3D case and is absent in the 2D case. We perform calculations both with and without this factor.

Our goal is to see whether a phase-only shaping of the wavepacket can produce substantial suppression of rovibrational dephasing. To consider control of this dephasing, it is crucial to define how the dephasing is *measured*. We follow [55] and we consider the frequency-gated fluorescence signal from the molecules. Note that this measurement is not resolved in the basis of eigenstates of the rovibrational Hamiltonian H_i - rather it is position-resolved. We can think of the contribution to the fluorescence signal from a given wavepacket $|\Psi_J(t)\rangle$ as the overlap between the wavepacket and a gate function $|\Phi_G\rangle = \sum_v g_{v,J}|vJ\rangle$. The gate is a function in space (ie: in the internuclear co-ordinate R) here given in the basis of the $|vJ\rangle$ wavefunctions. Since the form (in space) of the gate function should be exactly the same for all J, the amplitudes $g_{v,J}$ will be somewhat different for different values of J.

At this stage it is worth comparing the question posed here with the standard case of coherent control - e.g.: control of a chemical reaction. In the case where our measurement is resolved in the basis of the energy eigenstates, we can achieve phase-only control only via interference of multiple indistinguishable optical pathways [2]. Otherwise, spectral phases contribute only to phases in the various energy-eigenstate amplitudes, which have no effect when we make a measurement in this energy eigenstate-resolved basis (since only the modulus squared of the amplitudes will affect the measured yield in each eigenstate). This is the "emperor without clothes" argument in a 1989 paper by Brumer and Shapiro [59] - an apparent avenue for control which cannot, in fact, work.

Since we do not consider multiple interfering optical pathways, it might appear that one-photon phase-only control could not possibly work for our system. But since our measurement of the dephasing is *not* resolved in the energy eigenbasis, the above argument does not apply, and phase-only control is *in principle* achievable.

The overlap between $|\Psi_J(t)\rangle$ and $|\Phi_G\rangle$ is:

$$\begin{aligned} Q(J,t) &= \langle \Phi_G | \Psi_J(t) \rangle \\ &= \sum_v g^*_{vJ} a_{vJ} e^{-iE(v,J)t} \end{aligned} \tag{2.6}$$

The function $Q(J,t)$ characterises the electromagnetic field emitted by a molecule in a particular J-state, and the detected signal (the intensity of the emission) is proportional to $|Q(J,t)|^2$.

$$|Q(J,t)|^2 = \sum_v \sum_{v'} A_{vJ} A_{v'J} e^{-i\left\{\omega_J(v-v') - \omega_e x_e \left[\left(v+\frac{1}{2}\right)^2 - \left(v'+\frac{1}{2}\right)^2\right]\right\}t} \tag{2.7}$$

Where $A_{vJ} = g^*_{vJ} a_{vJ}$ are complex numbers, and the solely J-dependent terms in $E(v,J) - E(v',J)$ have cancelled. We now assume the rovibrational coupling is weak, and neglect the J-dependence of the A_{vJ} factors. This is equivalent to neglecting the rotational distortion of the vibrational wavefunctions for the duration of the pump pulse. However for the long-term evolution, we preserve the rovibrational distortion within the J-dependent *phase*, where the effect is accumulated over time. In place of A_{vJ} we have purely v-dependent constants $A_v = |A_v| e^{i\theta_v}$.

We assume that the intensity of the laser pulse which creates our wavepacket $|\Psi_J(t)\rangle$ on an excited electronic surface is in the weak-field (perturbative) regime. This assumption has two consequences. Firstly we may neglect the molecular alignment effect of the laser, since the aligning interaction energy will be $\ll kT$. This leaves the rotational density matrix in the form given above. This is to say that the rotational state of the molecules remains determined by the thermal Boltzmann distribution, and is not affected by the laser pulse. At higher intensities, the alignment effect would create a rotational wavepacket - in terms of our open system picture, this would mean that our control pulse would interact directly with both system and environment. Secondly, in the perturbative regime each eigenstate amplitude $|A_v| e^{i\theta_v}$ in the created wavepacket is proportional to the spectral amplitude of the laser field at the relevant transition frequency. For this reason, phase-only shaping of the laser pulse results *solely* in adjustment of the initial phases θ_v.

Since the spontaneous emission of molecules in different J-states is not coherent, the total fluorescence signal from the thermal ensemble of molecules is proportional to:

$$S(t) = \sum_{J=0}^{\infty} P(J) |Q(J,t)|^2 \tag{2.8}$$

$$= \sum_{J=0}^{\infty} \sum_v \sum_{v'} P(J) |A_v| |A_{v'}| e^{-i\left\{\theta_{v'} - \theta_v + \omega_J(v-v') - \omega_e x_e \left[\left(v+\frac{1}{2}\right)^2 - \left(v'+\frac{1}{2}\right)^2\right]\right\}t} \tag{2.9}$$

The qualitative behaviour of these functions can be summarised as follows. As the wavepacket moves between the inner and outer turning points,$|Q(J,t)|^2$ will oscillate with the average vibrational period $\omega_{\bar{v}} = \frac{\partial E}{\partial v}|_{v=\bar{v}}$. For nonzero anharmonicity ($\omega_e x_e > 0$) the wavepacket spreads over time. $|Q(J,t)|^2$ undergoes the well-known decay and revivals - including fractional revivals - as the $E(v,J)t$ phase factors for different v's

de- and re-phase with one another. In principle the J-dependent component of the phase evolution will also display revivals [52], but these will not in general coincide with the revivals due to anharmonicity. Thus the combination of anharmonic and rotational dephasing will typically result in a signal $S(t)$ which oscillates at the vibrational period, decaying over time without subsequent revival.

2.3.2 Phase-only shaping of the initial wavepacket: analytical estimates and numerical simulations

Consider the following term from equation (2.8)

$$E(v,J) - E(v',J) = \omega_J(v-v') - \omega_e x_e \left[\left(v+\frac{1}{2}\right)^2 - \left(v'+\frac{1}{2}\right)^2 \right] \tag{2.10}$$

Let us introduce $k = v - \bar{v}$, where $\bar{v}$ is the average v in the wavepacket. Then

$$\begin{aligned} E(v,J) - E(v',J) &= \tilde{\omega}_J(k-k') - \omega_e x_e \left(k^2 - k'^2\right) \\ \tilde{\omega}_J &= \omega_e - 2\omega_e x_e \left(\bar{v}+\frac{1}{2}\right) - \alpha_e J^2 = \omega_{\bar{v}} - \alpha_e J^2 \end{aligned} \tag{2.11}$$

Here $\omega_{\bar{v}}$ is the vibrational frequency at the average v.

To approximate the signal $S(t)$ analytically, we note that we are interested in the decay of the signal, not its oscillation with vibrational frequency. We then examine the behaviour of $|Q(J,t)|^2$ at discrete time intervals $t_N = \frac{2\pi N}{\omega_{\bar{v}}}$. At times $t = t_N$ we have

$$|Q(I,t_N)|^2 = \sum_{k=-\infty}^{k=\infty} \sum_{k'=-\infty}^{k'=\infty} A_k^2 A_{k'}^2 \exp\left\{ i \left[\theta_k - \theta_{k'} + t_N \omega_e x_e (k^2 - k'^2) - t_N \Delta\Omega (k-k') I \right] \right\} \tag{2.12}$$

Here $\bar{J}$ is the mean rotational state, $I = J - \bar{J}$, and $\Delta\Omega = -2\alpha_e \bar{J}$.

We now assume a Gaussian amplitude profile $A_k = e^{-k^2/2\sigma^2}$ and replace the sums over discrete states with an integral over continuous variables k and k'. One effect of this approximation is to remove the possibility of revivals, but this is acceptable since we are interested in the dephasing dynamics rather than the revivals. Now consider a Taylor expansion to second order of the initial phases: $\theta_k \simeq a + bk + ck^2$. The constant term has no effect since only relative phases between levels affect the signal. A linear chirp

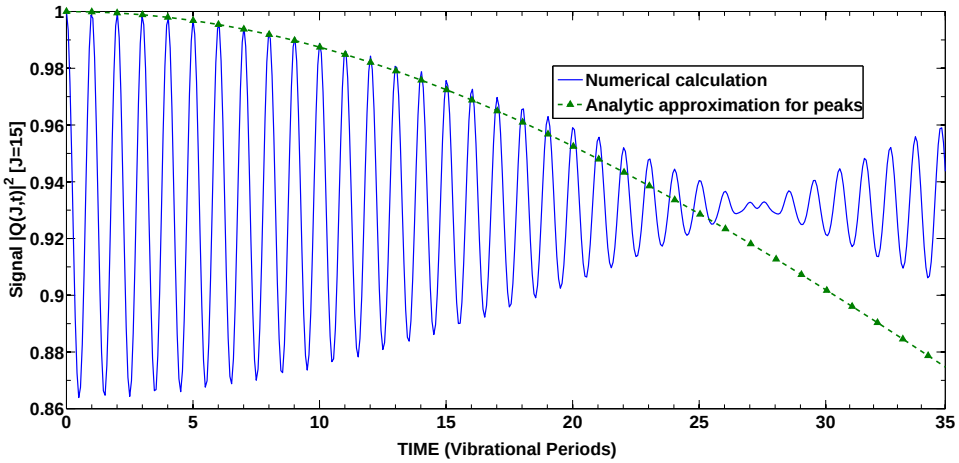


Figure 2.1: For the case of flat initial phases ($\theta_v = 0 \forall v$), the J=15 contribution to the signal $\frac{|Q(15,t)|^2}{max[|Q(15,t)|^2]}$ (solid blue line) is compared to the analytic approximation for the peaks $\tilde{Q}(J, NT)$ (dashed green line), where T is the vibrational period and N is an integer. The decay and revival of the single-J contribution seen here is due to the anharmonicity. The figure shows that while the approximation fails to capture the revival dynamics, it approximates the decay quite closely.

(bk) in the laser pulse spectrum is equivalent to a translation of the pulse in the time domain. Since we are interested in the behaviour of the molecule after the pulse, we must neglect this. As a result we assume that the initial phases have only quadratic dependence in the frequency domain (ie: linear chirp in the time domain), such that $\theta_k = ck^2$.

Completing the square in the exponent and performing the necessary Gaussian integrals yields

$$|\tilde{Q}(I, t_N)|^2 \propto e^{-\kappa(t_N)I^2} |\gamma(t_N)|^{-1} \tag{2.13}$$

$$\gamma(t_N) = \sigma^{-2} + i(\omega_e x_e t_N + c) \tag{2.14}$$

$$\kappa(t_N) = \frac{1}{2} |\gamma(t_N)|^{-2} (\Delta\Omega)^2 \sigma^{-2} t_N^2 \tag{2.15}$$

Figure 2.1 shows this approximation for the case of an unchirped initial wavepacket, showing its effectiveness in representing the decay in signal due to anharmonicity.

The form of $\tilde{Q}(I, t_N)$ provides insight into the dephasing mechanism, although the true behaviour of the signal is not revealed until we average over the J-distribution. First note that the parameter $|\gamma(t_N)|^2 = \sigma^{-4} + (\omega_e x_e t_N + c)^2$ can be viewed as a measure of wavepacket broadness in space. The σ^{-4} term captures the fact that a wavepacket in which few energy levels participate is broad in position space, while the $(\omega_e x_e t_N + c)^2$

term shows the anharmonic broadening and the effect of the chirp. Notice that $\gamma(0)$ is increased by either a positive or negative chirp: chirping the phases broadens the initial wavepacket. We also see that for a negative chirp, the anharmonicity will first *narrow* the wavepacket before broadening it. The wavepacket will be at its most narrow when $t_N = \frac{c}{\omega_e x_e}$.

In equation (2.13) we see that the broadness parameter $|\gamma(t_N)|^2$ appears both in the outer factor and within the exponential. The outer factor ensures that at any given time, a broader wavepacket will give a lower signal than a narrower one, since it will have a reduced overlap with the localised gate function. The role of $|\gamma(t_N)|^{-2}$ in the exponent is to decrease the instantaneous rate of decay of the signal for broader wavepackets. It may appear surprising that such decay occurs in $|\tilde{Q}(I, t_N)|^2$, because for a single rotational state $I = J - \bar{J}$ there is no dephasing. Recall that the times t_N are multiples of the *mean* vibrational period. For nonzero I, this is not the period that the wavepacket will actually move with. The decay in $|\tilde{Q}(I, t_N)|^2$ is due to this disparity.

For a given value of I, the signal for a broader wavepacket will decay more slowly over time. This can be understood by considering the extreme cases - a narrow δ-function-like peak (call this wavepacket $\Psi_N(R, t)$) and a broad wavepacket that is completely spread out along the classical trajectory (call this $\Psi_B(R, t)$). $\Psi_B(R, t)$ does not move along the trajectory as time increases, so its overlap with the gate function $\Psi_G(R)$ is small but constant. $\Psi_N(R, t)$ on the other hand, gives a strong signal when it is located on top of the gate function but if it is located away from the gate function then its overlap will vanish. So even a minor disparity between the wavepacket's period and the mean vibrational period will cause the signal for $\Psi_N(R, t)$ to decay.

Now we turn to the averaging over the J-distribution. Let $\beta = B_e/kT$. Substituting into equation (2.8) and again replacing the sum with an integral, we have

$$\tilde{S}(t_N) \propto |\gamma(t_N)|^{-1} \int_0^\infty dJ e^{-\beta J^2 - \kappa(t_N)(J-\bar{J})^2} \tag{2.16}$$

By completing the square in the exponent, we can rewrite this as follows:

$$\tilde{S}(t_N) \propto |\gamma(t_N)|^{-1} e^{-\kappa(t_N)\bar{J}(\bar{J}-J')} \int_0^\infty dJ e^{-(\beta+\kappa(t_N))(J-J')^2} \tag{2.17}$$

$$J' = \frac{\kappa(t_N)\bar{J}}{\beta + \kappa(t_N)} \tag{2.18}$$

The solution to the integral is expressed in terms of the complementary error function

$$\mathrm{erfc}(x) \propto \int_x^\infty dy e^{-y^2}$$

as

$$\tilde{S}(t_N) \propto |\gamma(t_N)|^{-1} e^{-\kappa(t_N)\bar{J}(\bar{J}-J')(\beta+\kappa(t_N))^{-\frac{1}{2}}} \mathrm{erfc}(-(\beta+\kappa(t_N))^{\frac{1}{2}} J') \tag{2.19}$$

Fig. 2.2 shows this analytic approximation, compared to the full $S(t)$ calculated numerically. Fig. 2.3 shows the result when the initial phases have a quadratic chirp $c = -0.1$.

The key result here is that in this model, contrary to the claim of Branderhorst et al. [55], negatively chirping the initial phases does not produce a wavepacket that is inherently resistant to the rovibrational dephasing. Instead we see that this produces an initially broadened wavepacket which is narrowed due to the anharmonicity, so that the signal first improves over time and subsequently decays. If there is no anharmonicity, this effect is not present.

We can study this effect qualitatively if we take the lower limit of the integral in equation (2.17) to $-\infty$. This approximation is justified since the factor $e^{-\kappa(t_N)J'^2}$ is small and goes quickly to zero as t_N increases. This yields

$$\tilde{S}_{-\infty}(t_N) = [(t_N - t')A + B]^{-\frac{1}{2}} \tag{2.20}$$

$$A = \beta(\omega_e x_e)^2 + \sigma^{-2}(\Delta\Omega)^2 \tag{2.21}$$

$$B = \beta(\sigma^{-4} + c^2) - At'^2 \tag{2.22}$$

$$t' = \frac{-\beta c \omega_e x_e}{A} \tag{2.23}$$

Since $t' \propto -c$, we can see the origin of the time-translation of the signal peak when a chirp is introduced. If we neglect the $\sigma^{-2}(\Delta\Omega)^2$ term in A, $t' = \frac{-c}{\omega_e x_e}$, which is the time at which the signal for a single value of I (or equivalently J) has its maximum, see equation (2.13). While this approximation to the signal is less accurate than equation (2.17), its behaviour is easier to understand. In this approximation the introduction of chirped initial phases simply time-shifts the entire signal. The behaviour of the numerically calculated

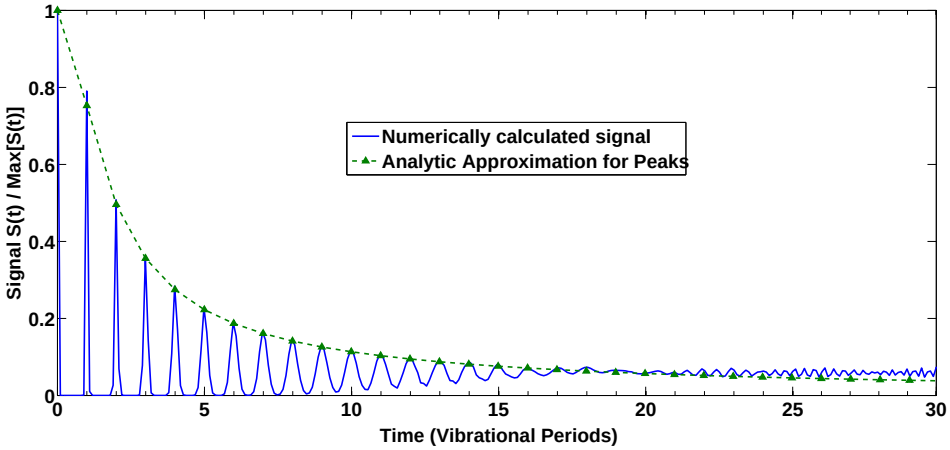


Figure 2.2: For the case of flat initial phases ($\theta_v = 0 \forall v$), the normalised signal function $\frac{S(t)}{max[S(t)]}$ (solid blue line) is compared to the analytic approximation for the peaks $\tilde{S}(NT)$ (dashed green line), where T is the vibrational period and N is an integer. The analytic approximation shows good qualitative agreement with the numerical results, demonstrating that the analytic approximation captures the decay of the signal due to rovibrational coupling.

$S(t)$ and the approximations $\tilde{S}(t_N)$ and $\tilde{S}_{-\infty}(t_N)$ are all qualitatively consistent. In this model, there is no sign of quadratically chirped phases providing any increase in inherent resistance to "decoherence", contrary to [55].

2.3.3 Phase- and amplitude-shaping: squeezed coherent wavepacket and two-state wavepacket

Branderhorst et al. [55] argue that initially position-squeezed wavepackets are more resistant to dephasing, since position-squeezed wavepackets are approximate eigenstates of the interaction Hamiltonian [53]. Although such a wavepacket is not position-squeezed at all times, it spends most of its time near the classical turning points, where it is position-squeezed. This section addresses whether this resistance to dephasing is observed in our model. In order to test this, we set the anharmonicity equal to zero and choose the initial vibrational wavepacket to be a squeezed coherent wavepacket displaced to the inner turning point. Creating such a wavepacket would require amplitude- and phase-modulation of the excitation pulse.

The complex amplitudes of each harmonic oscillator eigenstate in a squeezed coherent wavepacket $|\beta_c, \xi\rangle$ with displacement parameter β_c and squeezing parameter $\xi = |\xi| e^{i\phi_\xi}$, may be written in the form below [60], where $\mu = \cosh|\xi|$ and $\nu = e^{i\phi_\xi} \sinh|\xi|$. When the displacement $\beta_c = \pi$ and the squeezing factor ξ is real, we have the desired radially-squeezed wavepacket at the inner turning point (we take $\xi = 0.8$).

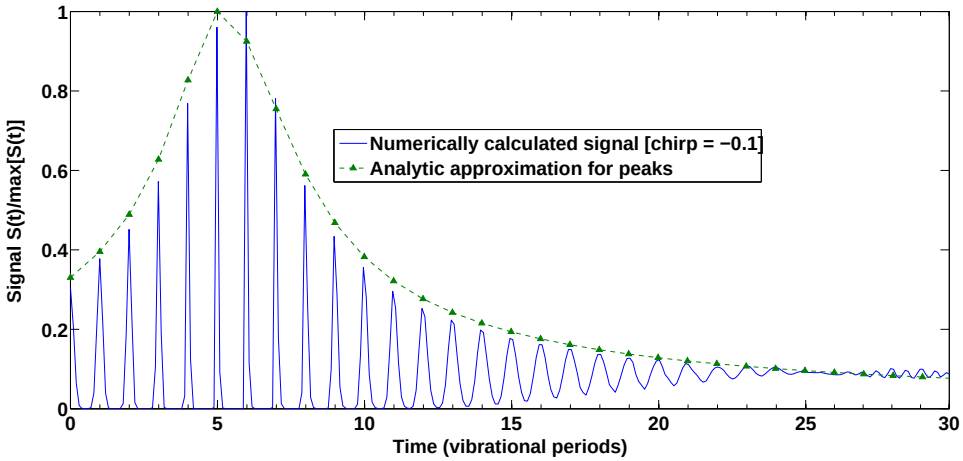


Figure 2.3: The same as Fig. 2.2, but with a negative quadratic chirp to the initial phases ($\theta_v = -0.1(v-\bar{v})^2$). Again there is good qualitative agreement - the analytic model shows a similar rise and fall.

$$A_n^c e^{i\theta_n^c} = \left(\frac{\nu}{2\mu}\right)^{\frac{n}{2}} \frac{1}{\sqrt{\mu n!}} \exp\left[-\frac{1}{2}\left(|\beta_c|^2 - \frac{\nu^*}{\mu}\beta_c^2\right)\right] H_n\left(\frac{\beta_c}{\sqrt{2\mu\nu}}\right) \tag{2.24}$$

We also consider the wavepacket $|\Psi_2\rangle = \frac{1}{\sqrt{2}}(|\bar{v}\rangle + |\bar{v}+1\rangle)$ containing only two adjacent vibrational levels, which will also show the beating at vibrational frequency. Figure 2.4 shows the signals calculated for the wavepacket with Gaussian amplitude profile and the squeezed coherent wavepacket. At a first glance, it appears that there is substantial difference in the surrogate measure of decoherence expressed by $S(t)$, for the three initial wavepackets. However, this first impression is incorrect. In order to assess their dephasing rate, the extrema of these curves are extracted and used to calculate a visibility $V = \frac{S_{\text{peak}} - S_{\text{valley}}}{S_{\text{peak}} + S_{\text{valley}}}$ for each period. This visibility is plotted as a function of time in Figure 2.5. Surprisingly, the three curves are nearly identical, showing no resistance to the dephasing process for the squeezed wavepacket $|\beta_c, \xi\rangle$ or the two-state wavepacket $|\Psi_2\rangle$.

The analytic work in the following sections is motivated by the need to explain why such drastic amplitude- and phase-adjustments of the initial wavepacket seem to have no effect on the dephasing process, contrary to the conclusions of [53] and [55].

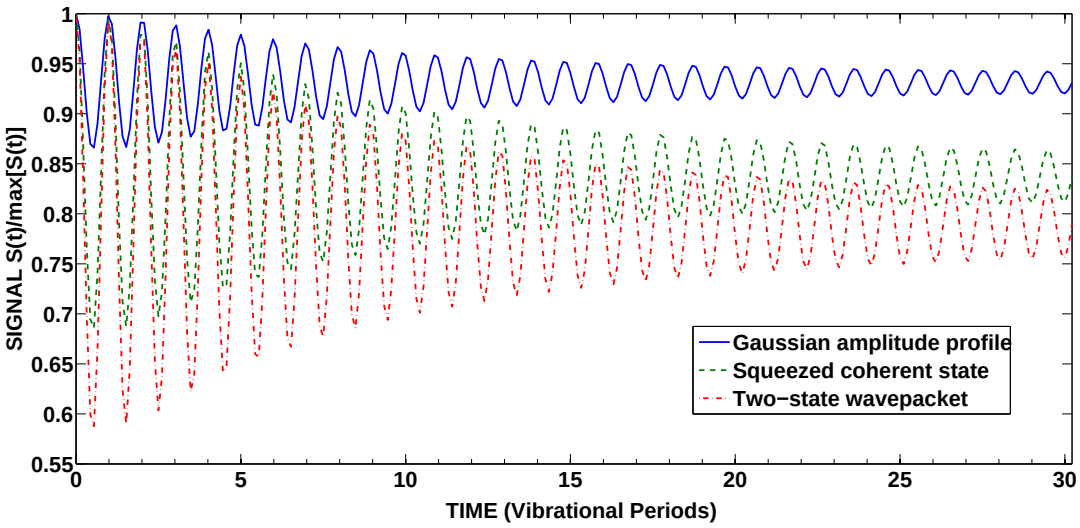


Figure 2.4: The normalised signals as a function of time for three different initial vibrational wavepackets. The first has a Gaussian amplitude profile $|\Psi_g\rangle = \sum_k e^{-k^2/2\sigma^2}|k\rangle$ (solid blue line), the second is a position-squeezed coherent wavepacket at the inner turning point $|\beta_c = \pi, \xi = 0.8\rangle$ (dashed green line) and the third is the wavepacket consisting of two adjacent vibrational states $|\Psi_2\rangle = \frac{1}{\sqrt{2}}(|\bar{v}\rangle + |\bar{v}+1\rangle)$ (dot-dashed red line). Here anharmonicity is zero, so the decay in the signal visibility is purely due to the rovibrational coupling.

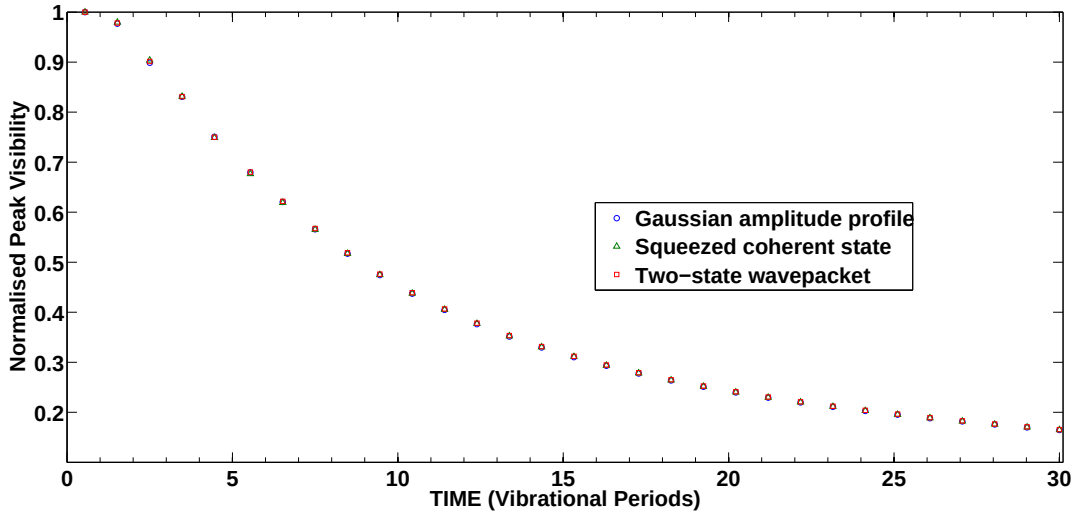


Figure 2.5: The normalised peak visibility $V/\max[V]$ as a function of time (extracted from Figure 2.4) for the three initial wavepackets $|\Psi_g\rangle$ (blue circles),$|\beta_c = \pi, \xi = 0.8\rangle$ (green triangles) and $|\Psi_2\rangle$ (red squares). This shows that for our model, these three different wavepackets show the same dephasing behaviour over time.

2.3.4 Analytical investigation of the signal function $S(t)$

Since we are interested solely in the dephasing due to thermal rotational population, for the following calculation we will neglect the anharmonicity $\omega_e x_e$. In contrast to the previous calculation, where we have looked at $S(t)$ at specific moments, here we will look at the complete time-dependence. The main approximation is to replace the summation over J with an integral. We perform the integral before the summation over v and v'. To simplify the J-integral, we shall assume that the bath distribution is $P(J) \propto 2Je^{\frac{-BJ^2}{kT}}$. We will also probe the dependence of $S(t)$ on the distribution of bath states by comparing the result for $P(J) \propto 2Je^{\frac{-BJ^2}{kT}}$ with that for the 2-D distribution $P_{2D}(J) \propto e^{\frac{-BJ^2}{kT}}$. The true 3-D thermal distribution, then, is proportional to the sum of these two distributions.

Performing the J-integral yields

$$S(t) \propto \sum_v \sum_{v'} A_v A_{v'} e^{-i\omega_e(v-v')t} \frac{1 + i\alpha_e J_0^2 (v-v')t}{1 + \alpha_e^2 J_0^4 (v-v')^2 t^2} \tag{2.25}$$

Here $J_0^2 = kT/B_e$ and $A_v = |A_v| e^{i\theta_v}$. Now we define time-dependent phases $\Phi_{vv'} = \omega_e(v-v')t - (\theta_v - \theta_{v'})$ (determined by the pure vibrational dynamics) and $\phi^\alpha_{vv'} = \arctan\left(\alpha_e J_0^2 (v-v')t\right)$ (determined by the dynamics due to rovibrational coupling). Then we may use the fact that $S(t)$ is real to write equation (2.25) in the following form:

$$S(t) \propto \sum_v \sum_{v'} |A_v||A_{v'}| \frac{1}{\sqrt{1 + \alpha_e^2 J_0^4 (v-v')^2 t^2}} \cos\left(\Phi_{vv'} - \phi^\alpha_{vv'}\right) \tag{2.26}$$

A first glance at equation (2.26) might suggest that the rovibrational coupling has little effect. The coherences between the levels with different $v \neq v'$ decrease as $\frac{1}{t}$ at long times and quadratically at short times. However, it is important to look closely at the effect of $\phi^\alpha_{vv'} = \arctan\left(\alpha_e J_0^2 (v-v')t\right)$ which enters the argument of the cosine.

Let Δv be the characteristic full width of the wavepacket in v. In addition, assume $\Delta v \gg 1$. Then we can separate three main timescales.

1) Short timescales $\Delta v \alpha_e J_0^2 t \ll 1$: In this case we have $\phi^\alpha_{vv'} \simeq \alpha_e J_0^2 (v-v')t$. Then, $\alpha_e J_0^2$ merely acts as a correction to the vibrational frequency ω_e, otherwise leaving the vibrational dynamics undisturbed:

$$S(t) \propto \sum_v \sum_{v'} |A_v||A_{v'}| \frac{1}{\sqrt{1+\alpha_e^2 J_0^4 (v-v')^2 t^2}} \cos\left[\omega_{J_0}(v-v')t - (\theta_v - \theta_{v'})\right] \tag{2.27}$$

Here $\omega_{J_0} = \omega_e - \alpha_e J_0^2$ is the rotationally-adjusted vibrational frequency. Maxima in $S(t)$ occur at times $t_n = \frac{2\pi n}{\omega_{J_0}}$.

2) Long timescales $\Delta v \alpha_e J_0^2 t \gg 1$: For this case, $\phi^\alpha_{vv'} \simeq \frac{\pi}{2}\text{sign}(v-v')$ becomes independent of v and the signal is given by

$$S(t) \propto S_0 + 2\sum_v \sum_{v'<v} |A_v A_{v'}| \frac{1}{\alpha_e J_0^2 |v-v'| t} \sin \Phi_{vv'} \tag{2.28}$$

Here $S_0 = \sum_v |A_v|^2$. Note that $\cos(\Phi_{vv'} - \phi^\alpha_{vv'})$ has been replaced with $\sin \Phi_{vv'}$, meaning that the maxima have shifted by $\frac{\pi}{2}$ compared to the very early times. The height of the maxima (thus also the contrast) is decreasing with time as $\frac{1}{t}$. Initial adjustments of θ_v can have *no* effect on the dephasing in this long-time limit, since the rovibrational coupling has disappeared from the phases completely. It remains only in the slowly decreasing envelope.

3) Intermediate timescales $\Delta v \alpha_e J_0^2 t \gtrsim 1$: $\phi^\alpha_{vv'}$ depends upon $v - v'$. Namely, for $v - v' = 1, 2$ we have $\phi^\alpha_{vv'} \lesssim 1$ and the maxima are at positions $t_n = \frac{2\pi n}{\omega_{J_0}}$. But for distant parts of the wavepacket, where $v - v'$ is large, we have a different situation, and $\phi^\alpha_{vv'} \simeq \frac{\pi}{2}$. So for different parts of the wavepacket, their contributions to $S(t)$ reach their maxima and minima at different times, and this reduces the overall contrast when we sum over v and v'. One can in principle compensate for this spread of maxima and minima with the initial phases θ_v. However, we will not be able to do so with a linear or quadratic chirp, since $\phi^\alpha_{vv'}$ is a non-linear function of $v - v'$.

2.3.5 Explanation for the Numerical Results of Section 2.3.3

At this stage we may reconsider the numerical results of Section 2.3.3, in particular Figure 2.5. Although the analytic results above do not address the visibility directly, we can ask whether they provide any qualitative explanation for the fact that the decay of visibility is the same for the three wavepackets (wavepacket with Gaussian amplitude profile $|\Psi_g\rangle$, the squeezed coherent wavepacket $|\beta_c, \xi\rangle$, and the wavepacket containing

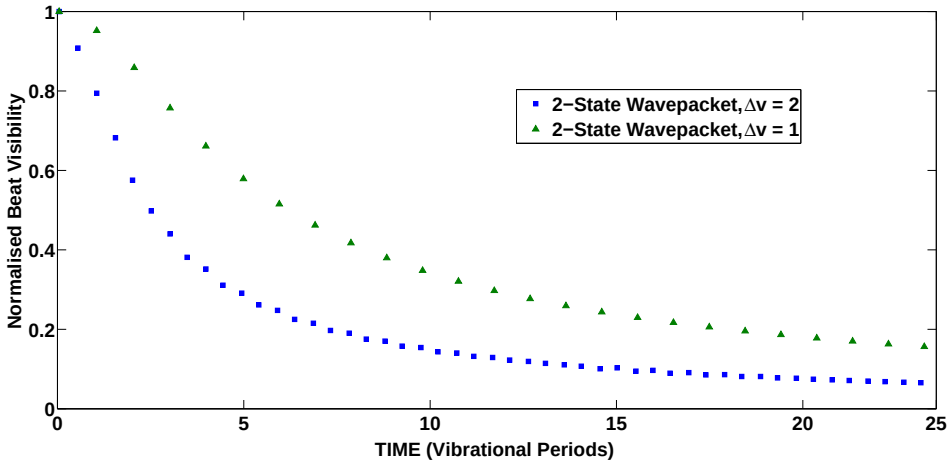


Figure 2.6: The normalised peak visibility $V/\max[V]$ as a function of time for two initial wavepackets, each containing only two vibrational states separated by Δv. Naturally, the case where $\Delta v = 2$ ($|\chi_2\rangle$) (blue squares) beats with twice the frequency of $\Delta v = 1$ ($|\Psi_2\rangle$) (green triangles) . We see that the dephasing behaviour over time is different for the two wavepackets, with the $\Delta v = 2$ wavepacket dephasing more rapidly than the wavepacket with $\Delta v = 1$. This demonstrates a case where *amplitude* modulation of the initial wavepacket has a significant effect on the dephasing dynamics.

only two adjacent states $|\Psi_2\rangle$). It is clear from examining equation (2.28) that the long-term behaviour of the wavepacket will be unaffected by the initial phases, and dominated by the terms in the sum where $v - v'$ is small. So for both $|\Psi_g\rangle$ and $|\beta_c, \xi\rangle$ the dominant dynamics is the beating between the mean $\bar{v}$ and adjacent states - the contribution from nearest-neighbour pairs away from the mean is suppressed due to the decay of the amplitudes A_v away from their maximum $A_{\bar{v}}$. At long timescales the behaviour of both of these wavepackets will be very similar to that of $|\Psi_2\rangle$. Note that for the parameter values used in the numerical simulation, which reflect the typical J_0^2 value in an experimental setup, the long-timescale limit $\Delta v \alpha_e J_0^2 t \gg 1$ is achieved after only a few vibrational periods. This provides a qualitative explanation for the form of Figure 2.5. Equation (2.28) also shows that while these three wavepackets behave similarly, the dephasing is not completely unaffected by amplitude modulation of the initial wavepacket. As an example we took another two-state wavepacket $|\chi_2\rangle = \frac{1}{\sqrt{2}}(|\bar{v}\rangle + |\bar{v}+2\rangle)$ and compared its dephasing to $|\Psi_2\rangle$in Figure 2.6. We see that this *amplitude* modulation has a substantial effect on the dephasing rate.

2.3.6 Dependence on the Bath Distribution

One question that is worth considering when looking at a model of environment-induced dephasing, is the following: how sensitively does the dephasing dynamics depend upon the exact distribution of population among the environment states? In order to address this question in our model, we repeat the calculation

of Section 2.3.4 using the 2-D rotational bath distribution $P_{2D}(J) \propto e^{\frac{-BJ^2}{kT}}$. Substituting this into equation (2.8) and approximating the sum as an integral as in (2.25), yields the following result (c.f. equation 2.26)

$$S(t) \propto \sum_v \sum_{v'} |A_v A_{v'}| (1 + \alpha_e^2 J_0^4 (v - v')^2 t^2)^{-\frac{1}{4}} \cos\left(\Phi_{vv'} - \tilde{\phi}_{vv'}\right) \tag{2.29}$$

Where $\tilde{\phi}_{vv'} = -\frac{1}{2}\phi^{\alpha}_{vv'}$ and all other quantities are defined as in Section 2.3.4 above. Therefore, changing the bath distribution alters the ro-vibrational dephasing angle from $\phi^{\alpha}_{vv'}$ to $\tilde{\phi}_{vv'}$ and changes the signal decay with time, so that at long times instead of decay $\propto \frac{1}{t}$ we have $\propto \frac{1}{\sqrt{t}}$. These changes - particularly the latter - are substantial. This result shows that here we have a very strong dependence of our outcome on the details of the environment states - namely the degeneracy of each J-level.

2.4 Conclusions

In this chapter we have studied rotationally-induced dephasing of vibrational wavepackets in hot diatomic molecules, with a view to establishing whether phase-only adjustments of the initial wavepacket can affect the rate of dephasing. An analytical investigation of the fluorescence signal $S(t)$ determined that there are three relevant timescales, determined by the size of the parameter $\Delta v \alpha_e J_0^2 t$. At short timescales, dephasing has not set in and there is no need to compensate for it. At long timescales, which can be reached after as little as a few vibrational periods in typical experiments, the dephasing process can no longer be compensated at all by initial wavepacket phases. Between these limits, there is an intermediate timescale where adjustments of the initial phases can, in principle, affect the dephasing rate.

The form for the signal $S(t)$ in equation (2.26) makes it clear that phase-only control of the dephasing means compensating for $\phi^{\alpha}((k-k'),t) = \arctan\left(\alpha_e J_0^2 (k-k')t\right)$ by selecting the values of the initial phases θ_k, where $k = v - \bar{v}$. At intermediate times we may no longer treat the arctan in ϕ^{α} as linear. Expanding it to third order we get $\phi^{\alpha}_{kk'} \simeq \alpha_e J_0^2 (k-k')t - \frac{1}{3}\alpha_e^3 J_0^6 (k-k')^3 t^3$, so we would need a cubic term in the phases to compensate for this. In our numerical simulations we have tried various values of cubic chirp in the initial phases, but none have reduced the dephasing rate. To explain the difficulties with phase-only control of the dephasing, let us assume that the initial phases are $\theta_k = bk + ck^2 + dk^3$. Then the phase $\Theta(k,k',t) = \Phi_{kk'} - \phi^{\alpha}_{kk'}$ in equation (2.26) can be written as follows (letting $n = k - k'$ and $m = k + k'$)

$$\begin{aligned}\Theta(n,m,t) &= F_0(n) + F_1(n)m + F_2(n)m^2 \\ F_0(n) &= \omega_e n - bn - \phi^\alpha(n,t) + \frac{1}{4}dn^3 \\ F_1(n) &= -cn \\ F_2(n) &= -\frac{3}{4}dn\end{aligned} \tag{2.30}$$

Now we assume that the constants A_k are Gaussian, i.e. $|A_k| = e^{-\frac{k^2}{k_0^2}}$. Then equation (2.26) gives

$$S(t) \propto \sum_n \sum_m \frac{e^{-\frac{n^2}{2k_0^2}}}{\sqrt{1+\alpha_e^2 J_0^4 t^2 n^2}} e^{-\frac{m^2}{2k_0^2}} \cos\left[F_0(n) + F_1(n)m + F_2(n)m^2\right] \tag{2.31}$$

The first thing to note is that the initial phases, which appear only inside the cosine, cannot affect the term $(1+\alpha_e^2 J_0^4 t^2 n^2)^{-\frac{1}{2}}$. So there is some overall decay in the signal which cannot be avoided by adjusting the initial phases. Secondly, examination of F_0 shows that the cubic chirp d can compensate for the rotational phase ϕ^α. However, the cubic chirp d *also* appears in F_2 - so when we perform the double sum over n and m, this introduces a further phase scrambling in addition to the thermal dephasing. It is clear from our analysis that phase-only suppression of the dephasing process is a challenging proposition, and even if it can be achieved, it can only operate over a limited timescale.

The question remains as to why our conclusions differ substantially from those of Branderhorst et al. [55], who reported control of the dephasing process by application of quadratically-chirped excitation pulses. The key assumption in our model is neglecting the effect of rotational distortion of the vibrational wavefunctions during the pump pulse, i.e. neglecting the J-dependence of the A_{vJ} factors in equation (2.7). It might still be possible that phase-only control can be achieved if these distortions are taken into account. If this were to be shown to have an effect on the results, it would mean that the excitation pulse in the experiment was creating a fully rovibrational wavepacket, i.e. the control pulse would be directly interacting with both the system and environment dynamics. In such a case, we cannot view the pulse as creating a vibrational ("system") wavepacket which is resistant to the effect of the rotational ("environment") dynamics, but rather the experimenter would be altering both system and environment with the initial pulse. For the open system formalism, and statements about protection from dephasing or "decoherence", to make sense, we must consider a control pulse that only affects the system.

Chapter 3

Suppression of rovibrational dephasing by nonlinear resonance

3.1 Introduction to nonlinear resonance

Nonlinear resonance is a well-known phenomenon that occurs in both classical and quantum systems [61]. It occurs in systems with weak anharmonicity (examples of such quantum systems include Rydberg states of hydrogen atoms [61] and diatomic molecules with Morse oscillator potentials [1]), when driven by a sufficiently strong driving force. It is "nonlinear" because it results from the anharmonicity (i.e. quadratic term) in the energy levels, and it is "resonance" because it occurs when the driving force is resonant with a particular transition between two adjacent levels.

One effect of nonlinear resonance is to create a "stable island" in the classical phase space, allowing one to initiate quantum wavepackets or ensembles of classical trajectories which are resistant to anharmonic dephasing by placing them onto the stable island. This process is explained and analytically derived in Section 3.3 below. Shapiro et al. [1] have shown theoretically that the nonlinear resonance effect can be used to suppress rovibrational dephasing in diatomic molecules. In this chapter, we briefly summarise the way in which this suppression occurs, and extend the work of Shapiro et al. by considering the case where the molecule is driven not by a continuous-wave two-colour laser field, but by a sequence of laser pulses. In this case, it transpires that nonlinear resonance provides a powerful tool for suppressing rovibrational dephasing, and also for controlling vibrational wavepacket dynamics in a number of ways, described in Section 3.3.1.

In a homonuclear diatomic molecule, the driving force on the molecule is achieved via the dynamic

Stark shift, which is explained in Section 3.2. In this case, the laser frequency of the driving field is far *away* from resonance with any vibrational transition. At first, this may appear to ruin one's chances of achieving nonlinear resonance. In fact, however, the nonlinear resonance is achieved because the delay between successive pulses in the pulse train (or in the case described in [1], the beat period of the two-colour field) is tuned at or near resonance with a particular vibrational transition.

3.2 The dynamic Stark shift

The dynamic Stark shift is the alteration of the molecular potential energy surface (of a particular electronic state) by off-resonant light. It provides a mechanism for controlling the vibrational degree of freedom with an external light field. As a result it offers a potential avenue for experimental control of rovibrational dephasing. What follows is a standard treatment of the dynamic Stark shift, and loosely follows that in Chapter 4 of reference [62]. We assume that the molecule is initially in the vibrational and electronic ground state. For simplicity, the derivation here is performed in one dimension. The Hamiltonian is given by:

$$\begin{aligned} \hat{H} &= \hat{H}_0 + \hat{V} \\ \hat{V} &= \hat{\mathbf{d}} \cdot \mathbf{E}(\mathbf{t}) = \frac{\mathbf{1}}{\mathbf{2}} \hat{\mathbf{d}} \left(\mathbf{F}(\mathbf{t}) \mathbf{e}^{\mathbf{i}\omega\mathbf{t}} + \mathbf{F}^*(\mathbf{t}) \mathbf{e}^{-\mathbf{i}\omega\mathbf{t}} \right) \end{aligned} \tag{3.1}$$

Here we assume that the laser frequency ω is off-resonant with both the vibrational and electronic transitions. Now we apply the usual perturbation theory, so that the solution for the state of the molecule at time t is $|\psi\rangle \simeq |\psi^{(0)}\rangle + |\psi^{(1)}\rangle + |\psi^{(2)}\rangle$, such that the Schrödinger equation gives

$$\begin{aligned} i\partial_t |\psi^{(0)}\rangle &= \hat{H}_0 |\psi^{(0)}\rangle \\ i\partial_t |\psi^{(1)}\rangle &= \hat{H}_0 |\psi^{(1)}\rangle + \hat{V} |\psi^{(0)}\rangle \\ i\partial_t |\psi^{(2)}\rangle &= \hat{H}_0 |\psi^{(2)}\rangle + \hat{V} |\psi^{(1)}\rangle \end{aligned} \tag{3.2}$$

If we assume that the molecule starts in the vibrational and electronic ground state $|0>$ and define the energy of this state as the zero of our energy scale, then $|\psi^{(0)}\rangle = |0\rangle$ for all times. Expanding the solution in the basis of energy eigenstates yields $|\psi\rangle = \sum_k c_k |k\rangle$ and similarly for the first and second order corrections, $|\psi\rangle^{(1)} = \sum_k c_k^{(1)} |k\rangle$ and $|\psi\rangle^{(2)} = \sum_k c_k^{(2)} |k\rangle$. Solving equation (3.2) for $c_k^{(1)}(t)$ gives

$$c_k^{(1)} = -i \int_{-\infty}^{t} dt' e^{-i\omega_k t'} V_{k0}(t') \tag{3.3}$$

Here ω_k is the energy of the kth eigenstate and V_{k0} is the interaction matrix element $V_{k0}(t) = d_{k0}E(t) = \langle k|\hat{d}|0\rangle \frac{1}{2}E(t)$. If we assume that the amplitude envelope of the electric field varies slowly in comparison to the oscillation of the field at the laser frequency (ie: $\frac{1}{F(t)}\frac{dF(t)}{dt} \ll \omega \ \forall t$), then the following approximation for $c_k^{(1)}$ is valid:

$$c_k^{(1)} = -\frac{1}{2} i d_{k0} \left[F(t) \frac{e^{-i(\omega_k+\omega)t}}{i(\omega_k+\omega)} + F^*(t) \frac{e^{-i(\omega_k-\omega)t}}{i(\omega_k-\omega)} \right] \tag{3.4}$$

This solution can be substituted into the Schrödinger equation for $\dot{c}_k^{(2)}$ to give

$$\dot{c}_k^{(2)} = \sum_j -\frac{1}{4} e^{-i\omega_k t} d_{kj} d_{j0} \left(|F(t)|^2 \left[\frac{1}{\omega_j - \omega} + \frac{1}{\omega_j + \omega} \right] + [F(t)]^2 \frac{e^{-i2\omega t}}{\omega_j + \omega} + [F^*(t)]^2 \frac{e^{i2\omega t}}{\omega_j - \omega} \right) \tag{3.5}$$

Now we make the rotating-wave approximation and discard the fast-oscillating terms with frequency 2ω. As we look at the time derivative of the ground state amplitude ($\dot{c}_0 = \dot{c}_0^{(0)} + \dot{c}_0^{(1)} + \dot{c}_0^{(2)}$), noting that by symmetry $d_{00} = 0$, we see that:

$$\begin{aligned} i\dot{c}_0 &= -\frac{1}{4} \alpha_{00} |F(t)|^2 \\ \alpha_{00} &= \sum_j d_{0j} d_{j0} \left(\frac{1}{\omega_j - \omega} + \frac{1}{\omega_j + \omega} \right) \end{aligned} \tag{3.6}$$

Thus, the ground state potential energy surface $V(R)$ experiences a laser-induced time-dependent shift equal to $\Delta V(R,t) = -\frac{1}{4}|F(t)|^2 \alpha_{00}(R)$. We can think of α_{00} as the molecular polarizability. The dipole moments d_{0j} and transition frequencies ω_j depend on the internuclear separation R, and thus so does the polarizability $\alpha = \alpha(R)$. This dynamic Stark shift can be thought of as caused by virtual transitions from the ground electronic state to an excited electronic state and then back to the ground state. Note that the dynamic Stark shift potential $\Delta V(R,t) = -\frac{1}{4}|F(t)|^2 \alpha_{00}(R)$ depends on the *envelope* $|F(t)|^2$ of the laser field and not on the oscillating field itself. From the above, it is clear that an external, off-resonant laser field can

be used to make a time-dependent alteration $\Delta V(R,t)$ to the molecular potential energy surface and thus control vibrational motion within the molecule.

3.3 Nonlinear resonance: diatomic molecule driven by pulse train

Now we consider the dynamics of a diatomic molecule driven by a train of laser pulses.Consider the vibrational motion of a molecule in a given electronic state $|i\rangle$ subject to a laser field $E(t) = F(t)\cos(\omega_L t)$ where $F(t)$ is a slowly-varying envelope and the laser frequency ω_L is off-resonant with vibrational and electronic transitions. Then, due to the dynamic Stark shift (see Section 3.2), the vibrational Hamiltonian is

$$\begin{aligned} \hat{H} &= \hat{H}_0 + \hat{V}_L \\ \hat{H}_0 &= \frac{\hat{p}^2}{2\mu} + U_i(\hat{R}) \\ \hat{V}_L &= -\frac{1}{4}\alpha(\hat{R})F^2(t) \end{aligned} \tag{3.7}$$

Here $\hat{p}$ is the momentum operator, $\hat{R}$ is the internuclear co-ordinate operator, U_i is the molecular potential energy surface and α the polarizability of the molecule in the electronic state $|i\rangle$. If we assume that the envelope $F(t)$ is that of a pulse train with period $T = \frac{2\pi}{\Omega}$, the pulse-train having an overall slowly-varying envelope $f(t)$, then we may write $F^2(t)$ as

$$F^2(t) = f^2(t)\sum_{k=1}^{\infty} F_k^2 \cos(k\Omega t) \tag{3.8}$$

We assume that each pulse in the train can be shaped as desired, which is to say the coefficients F_k^2 of each harmonic of the fundamental frequency Ω are under the experimenter's control. Consider a vibrational wavepacket $|\Psi(t)\rangle$ expanded in the basis of vibrational eigenfunctions $|v\rangle$ with energies E_v. If the wavepacket is centred on some average $v = \bar{v}$ and Ω is tuned near to resonance with the vibrational frequency of the level $\bar{v}$, then it is convenient to write the wavepacket in the following form, anticipating the rotating-wave approximation:

$$|\Psi(t)\rangle = e^{-iE_0 t} \sum_m C_m e^{-im\Omega t} |m\rangle \tag{3.9}$$

Here $m = v - \bar{v}$. For convenience we are now counting levels from $\bar{v}$, so that the level $|m\rangle$ (with relabelled energy E_m) would previously have been labelled $|\bar{v} + m\rangle$ (with energy $E_{\bar{v}+m}$). The Schrödinger equation then yields the following equation for $C_m(t)$:

$$i\dot{C}_m = \Delta_m C_m - \frac{1}{4} f^2(t) \sum_{k=1}^{\infty} F_k^2 \cos(k\Omega t) \sum_{m'} e^{-i(m'-m)\Omega t} \alpha_{m,m'} C_{m'} \tag{3.10}$$

Here the detunings are $\Delta_m = E_m - E_0 - m\Omega$ and the matrix elements are $\alpha_{m,m'} = \langle m|\alpha(\hat{R})|m'\rangle$.

Let us consider the matrix elements $\alpha_{m,m'}$ of the polarizability, using the example of a harmonic oscillator. In a quantum harmonic oscillator (placing the equilibrium distance at $R_{eq} = 0$ for simplicity), the operator that couples adjacent vibrational states is $\propto \hat{R}$, since $\hat{R} \propto (a^\dagger + a)$, where a and $a^\dagger$ are the creation and annihilation operators for vibrational quanta). Operators $\propto \hat{R}^2$ couple each state to itself and to states two levels away from it, and so on for increasing powers of $\hat{R}$. Consider a Taylor expansion of the polarizability about the equilibrium position ($R = 0$):

$$\alpha(\hat{R}) = \alpha^{(0)} + \alpha^{(1)}\hat{R} + \alpha^{(2)}\hat{R}^2 + ... \tag{3.11}$$

Where the $\alpha^{(0)}$, $\alpha^{(1)}$ etc. are constant complex coefficients. The value of any particular matrix element $\alpha_{m,m'}$ for a harmonic oscillator depends entirely upon $k = |m - m'|$ and the coefficients $\alpha^{(0)}$, $\alpha^{(1)}$ etc. For a weakly anharmonic oscillator, these considerations still apply. Furthermore, it is reasonable to assume ([1]) that for a homonuclear diatomic molecule (modelled as a Morse oscillator), $\alpha^{(1)} >> \alpha^{(n>1)}$, i.e. that the dependence of the polarizability on R (the internuclear distance measured from the equilibrium position) is close to linear.

Continuing our derivation from equation (3.10), we let $\alpha_{m,m+k} = \alpha_{m,m-k} = \alpha_k$ and make the rotating-wave approximation, retaining only the time-independent terms in equation (3.10), yielding:

$$i\dot{C}_m = \Delta_m C_m - \frac{1}{8} f^2(t) \sum_{k=1}^{\infty} \alpha_k F_k^2 \left(C_{m+k} + C_{m-k}\right) \tag{3.12}$$

Now, to gain insight into the dynamics of this system, we try to find another, well-understood, quantum system with the same equation of motion. Consider a rigid rotor in a plane, with the following (time-independent) Hamiltonian:

$$\begin{aligned} H &= B\hat{M}^2 + V(\phi) \\ V(\phi) &= -\sum_{k=1}^{\infty} V_k \cos\left(k\phi\right) \end{aligned} \tag{3.13}$$

Here B is the rotational constant, $\hat{M} = -i\frac{\partial}{\partial\phi}$ is the angular momentum operator with eigenstates $|M\rangle = \frac{e^{iM\phi}}{\sqrt{2\pi}}$. Consider a rotational wavepacket $|\chi\rangle$ centred on the rotational eigenstate $|M_0\rangle$. Let us write this rotational wavepacket in a form similar to the way we expressed the vibrational wavepacket (equation (3.9) above):

$$|\chi\rangle = e^{iBM_0^2 t} \sum_N C_N(t) \frac{e^{i(M_0+N)\phi}}{2\pi} \tag{3.14}$$

Now, noting that $\int_0^{2\pi} d\phi e^{i(P-Q)\phi} = \delta_{P,Q}$, it is straightforward to show that the Schrödinger equation yields the following equation for the coefficients C_N:

$$i\dot{C_N} = \Delta_N C_N - \sum_{k=1}^{\infty} \frac{V_k}{2} \left(C_{N+k} + C_{N-k}\right) \tag{3.15}$$

Here $\Delta_N = \left(B(M_0+N)^2 - BM_0^2\right) = B(N^2 + 2M_0 N)$. This is indeed very close to our original equation of motion for the driven molecule, equation (3.12). If our mapping from the vibrational motion of the molecule to the rotor picture is to work, then we need Δ_N to have the same dependence on N as the detuning Δ_m has on m.

Suppose the molecule has the following anharmonic energy spectrum:

$$E_m = E_0 + \omega_0 m + \kappa m^2 \tag{3.16}$$

Then the detunings are:

$$\Delta_m = E_m - E_0 - m\Omega = m(\omega_0 - \Omega) + \kappa m^2 \tag{3.17}$$

These indeed have the same form as $\Delta_N = B(N^2 + 2M_0 N)$, up to notation. Therefore we can map the pulse-train-driven vibrational motion to the motion of a rigid rotor in a time-independent potential, if we make the following identifications:

$$\begin{aligned} B &= \kappa \\ M_0 &= \frac{\omega_0 - \Omega}{2\kappa} \\ V_k &= \frac{1}{4} f^2(t) \alpha_k F_k^2 \end{aligned} \tag{3.18}$$

Note that the Hamiltonian in the rotor picture is not strictly time-independent, since the potential $V(\phi)$ will change in time due to the envelope $f(t)$ of the entire pulse train. However, this envelope is assumed to be an arbitrarily slowly-varying function of time, so we may make the adiabatic approximation and simply treat the "slow" time (i.e. the argument of $f(t)$) as a parameter when we map from the vibrational motion to the rotational motion.

Now we must identify the meaning, in terms of the driven vibrational motion, of the angle co-ordinate ϕ in the rotor picture. It can be shown ([1],[48]) that in the semiclassical limit (where the central vibrational level in the wavepacket, $\bar{v}$, is large), the phase ϕ is equivalent to the classical phase (the variable conjugated to the classical action) along the vibrational orbit, measured *relative* to the fixed point of the resonance, which moves around the orbit with the driving frequency Ω, i.e. $\phi = \varphi - \Omega t$ where φ is the classical phase. This means that a highly-localised stationary state in the rotor picture is equivalent to a non-spreading vibrational wavepacket moving around the classical orbit at frequency Ω.

But since we have not specified the actual form of the potential $V(\phi)$, we cannot be sure whether such localised stationary states exist, and thus how and whether a non-spreading vibrational wavepacket may be

created. Consider first the case where $\alpha_1 F_1^2 >> \alpha_k F_k^2$ for all $k > 1$. As mentioned earlier in this section, this approximation holds as long as the R-dependence of the polarizability $\alpha(R)$ is linear (or at least, the linear term dominates).

Then the potential in the rotor picture is $V(\phi) \simeq -V_1 \cos(\phi)$. This is a "bucket" potential with a minimum at $\phi = 0$, equivalent to placing a dipole rotor in a static electric field, and mathematically the problem the reduces to that already discussed by Shapiro et al. [1]. If V_1 is sufficiently large, the bucket will contain bound states, and since the potential near the minimum is approximately harmonic, these will resemble the harmonic oscillator eigenfunctions. As such, the ground-state eigenfunction of the bucket will resemble a Gaussian with its centre at $\phi = 0$ - which is a localised stationary state, as required. If the driving field is switched on adiabatically, this eigenstate will evolve from the $M_0 = 0$ free rotor eigenstate as the field is switched on. Examining equation (3.18) we see that $M_0 = 0$ so long as $\omega_0 - \Omega \simeq 0$, ie: the driving field is perfectly tuned to resonance with the vibrational frequency of the level $\bar{v}$. As long as this resonance condition holds, the initial vibrational wavepacket will evolve into a non-spreading wavepacket locked in phase to the driving frequency Ω.

3.3.1 Control of vibrational dynamics via nonlinear resonance

Consider now the case where the pulse train is resonant with the vibrational frequency of a level on an *excited* electronic state, and at some time t_0 an excitation pulse (of very short duration compared to the pulse train period $T = \frac{2\pi}{\Omega}$) creates a wavepacket on the excited electronic potential energy surface via Frank-Condon excitation from the ground electronic state. Here we treat $f(t)$ as a constant, ie: the pump pulse arrives when the train of control pulses is already turned on and so the wavepacket is subject to the full external potential as soon as it is excited, rather than being subject to an adiabatically changing potential. We assume that the potential energy surfaces are shaped such that the wavepacket created at $t = t_0$ is initially localised at the inner turning point. Now we may switch to the rotor picture and ask what sort of initial wavepacket will be created. Since the angle ϕ is identified with the classical phase relative to the stable point of the resonance, and the stable point moves around the classical orbit at the driving frequency, the initial wavepacket will be localised around a particular angle ϕ_0 determined by the excitation time t_0.

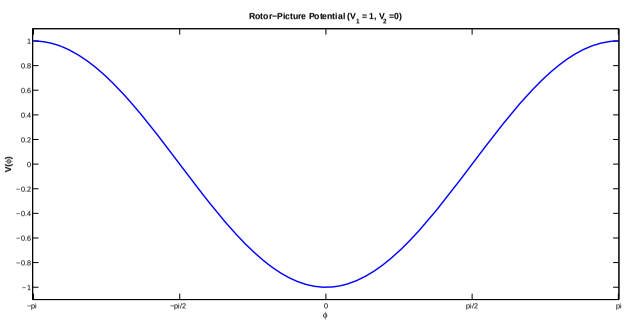
If $t_0 = \frac{2\pi n}{\Omega}$ where n is an integer, then at $t = t_0$ the stable point is located at the inner turning point, and the wavepacket in the rotor picture will be centred at $\phi_0 = 0$. If $V(\phi) \simeq -V_1 \cos(\phi)$ as above, this rotational wavepacket will be confined by the potential well at $\phi = 0$, and (moving back to the vibrational motion picture) we know that our vibrational wavepacket will not spread, and will be locked in phase with

the driving field. If $t_0 = (N + \frac{1}{2})T$ then the stable point of the resonance will be at the *outer* turning point. So in the rotor picture, the wavepacket will be centred at $\phi_0 = \pi$, at the maximum of the potential $V(\phi)$. Such a wavepacket is not confined by the potential $V(\phi)$ and so corresponds to a vibrational wavepacket which is *not* phase-locked to the driving field. There are interesting cases in between, where the rotor-picture wavepacket will "slosh" from one side of the potential bucket to the other as time passes. This results in a vibrational wavepacket that oscillates around the stable point of the resonance (Shapiro et al. [1] show that such vibrational wavepackets in a resonantly-driven molecule can store quantum information in a way resistant to rovibrational dephasing). Simply by controlling the excitation time t_0, we may create an initial rotor-picture wavepacket that is localised around any value of ϕ_0 that we choose.

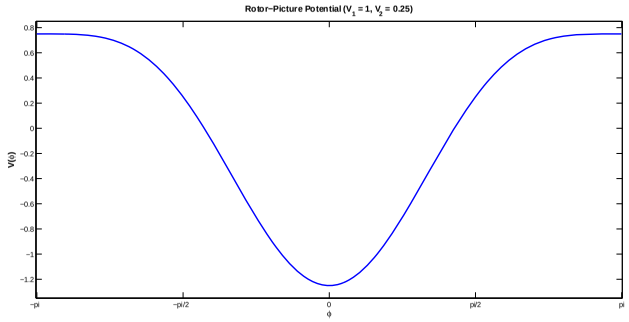
Figure 3.1 shows some example rotor-picture potentials produced by varying the amplitudes of V_1 and V_2. The figure shows the possibility to control the properties of the nonlinear resonance by shaping the pulse train. Shaping of the pulse train (i.e. adjustment of the F_k^2's) controls the V_k's, which in turn controls the number, position, and depth of potential wells in the rotor-picture potential $V(\phi)$. Such wells in $V(\phi)$ correspond to regions of the classical trajectory (in the frame rotating with frequency Ω) where non-spreading wavepackets can be created. The depth of a given well controls how tightly the wavepacket will be localised along the classical trajectory. This control, combined with the control of the initial wavepacket in the rotor-picture, allows substantial control over vibrational dynamics.

3.3.2 Suppression of dephasing via nonlinear resonance

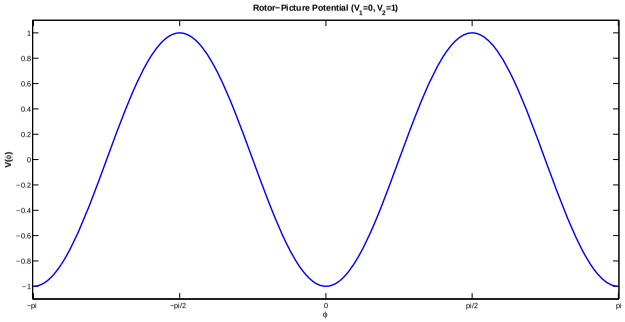
Shapiro et al. [1] show that nonlinear resonance can be used to reduce or remove the effects of rovibrational dephasing on a vibrational wavepacket. If we introduce rovibrational coupling, the vibrational frequency ω_0 will now depend on the rotational quantum number J of the molecule, $\omega_J = \omega_0 - \alpha_e J(J+1)$ where α_e is the rovibrational coupling constant. If we consider a molecule in a particular J-state, the derivation from Section 3.3 proceeds identically, but with ω_0 replaced by ω_J throughout. If we have an ensemble of rotationally-hot molecules, so that the value of J follows a thermal distribution $P(J)$, the result is that we have an incoherent distribution of values of ω_J. What does this mean in the rotor picture? Looking at equation (3.18) we have that $M_0 = \frac{\omega_J - \Omega}{2\kappa}$, so incoherent population of J-states corresponds to incoherent population of excited states in the rotor picture. Assuming that $V(\phi)$ possesses a potential well (e.g. the well at $\phi = 0$ for $V(\phi) = -V_1 \cos(\phi)$), Shapiro et al. point out that incoherent population of J-states will have no effect on the dynamics if the resulting spread in rotor-picture energy BM_0^2 is below the zero-point energy of the well. Then the vibrational wavepackets of molecules with varying J-states will all correspond



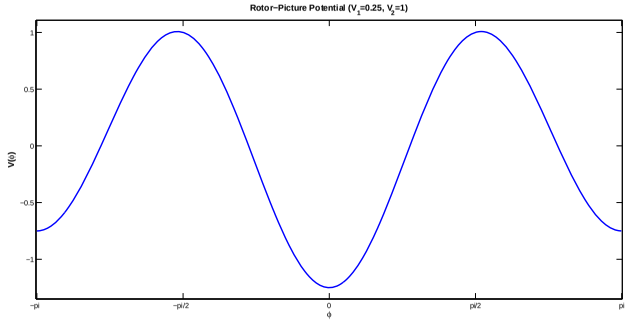
(a) $V(\phi) = -\cos(\phi)$



(b) $V(\phi) = -\cos(\phi) - 0.25\cos(2\phi)$



(c) $V(\phi) = -\cos(2\phi)$



(d) $V(\phi) = -0.25\cos(\phi) - \cos(2\phi)$

Figure 3.1: Rotor-picture potential energy as a function of the angle ϕ, $V(\phi) = -V_1\cos(\phi) - V_2\cos(2\phi)$, for example values of V_1 and V_2. In terms of the driven vibrational motion, ϕ corresponds to the classical phase (conjugated to the action) relative to the stable point of the nonlinear resonance, and the coefficients V_k are determined by the envelope of the driving field and the matrix elements of the molecular polarization [see equations (3.7), (3.8) and (3.18)]. Fig. 3.1(a) shows the case where $V_1 = 1$ and $V_2 = 0$ with a minimum at $\phi = 0$ which can be used to create a non-spreading wavepacket locked in phase to the driving field. In Fig. 3.1(b), $V_1 = 1$ and $V_2 = 0.25$. Note that the addition of the weak V_2 contribution deepens the potential well at $\phi = 0$. In Fig. 3.1(c), $V_1 = 0$ and $V_2 = 1$, giving a double-well potential with minima at $\phi = 0, \pi$. In Fig. 3.1(d), $V_1 = 0.25$ and $V_2 = 1$, and the addition of a weak V_1 results in the two potential wells having different depths. These example cases illustrate the kind of control that may be exerted over the form of the rotor-picture potential, and thus over the effects of the nonlinear resonance on the vibrational wavepacket dynamics.

to the ground state of the rotor-picture potential well, resulting in identical wavepackets phase-locked to the driving field.

For $V(\phi) = -V_1 \cos(\phi)$, Taylor expansion to second-order around $\phi = 0$ allows an approximation of the zero-point energy of the well. Assuming that the pulse train frequency Ω is resonant with some state $|\bar{v}, \bar{J}\rangle$, then, calling the range of detunings due to the J-distribution $\langle\Delta\omega\rangle$, the condition for complete suppression of dephasing is

$$\langle\Delta\omega\rangle < 2^{\frac{1}{4}} \kappa^{3/4} V_1^{\frac{1}{4}} \tag{3.19}$$

If we include a term $-V_2 cos(2\phi)$, the potential well at $\phi = 0$ is deepened (see Figure 3.1), and the above condition becomes:

$$\langle\Delta\omega\rangle < 2^{\frac{1}{4}} \kappa^{3/4} \left(V_1 + 4V_2\right)^{\frac{1}{4}} \tag{3.20}$$

Assuming that the V_k's for $k > 2$ are negligible due to the matrix elements α_k of the polarizability (i.e. assuming that $\alpha(R) = \alpha(\hat{R}) = \alpha^{(0)} + \alpha^{(1)}\hat{R} + \alpha^{(2)}\hat{R}^2$), we see that use of a pulse train can substantially improve the dephasing suppression compared to the continuous-wave case. If $V_1 < 4V_2$, then a second rotor-picture potential well is created at $\phi = \pi$, which could also be used to suppress the effects of dephasing. The condition for suppression in the second well is:

$$\langle\Delta\omega\rangle < 2^{\frac{1}{4}} \kappa^{3/4} \left(4V_2 - V_1\right)^{\frac{1}{4}} \tag{3.21}$$

Recall that $V_k = \frac{1}{4} f^2(t) \alpha_k F_k^2$, so we can control the values of V_1 and V_2 by adjusting the pulse train envelope, and thus F_1^2 and F_2^2. For example, we can make $F_1^2 << F_2^2$ by doubling the frequency of the pulses in the train. So by shaping the pulse train, the experimenter has control over the degree of dephasing suppression that is achieved in each potential well in the rotor picture, or equivalently, each stable island in the classical phase space of the diatomic molecule's vibration.

To connect this work to the methods of decoherence suppression discussed in Section 1.3, I would first note that the nonlinear resonance approach does not correspond to a "bang-bang" control (Section 1.3.3),

since the applied pulse train is *resonant* with the molecular vibration. The hallmark of bang-bang control is to use a control pulse which operates on a much faster timescale than the characteristic timescale of the system dynamics. In the above model, the dephasing suppression can be made "perfect", i.e. if the rotor picture excitations are below the ground state energy of the potential well, then the thermal distribution of J-states can have *no* effect on the molecule's vibrational dynamics while the driving field is present. I would therefore speculate that this method is most conceptually similar to a dynamical decoupling scheme, whereby the control field creates a decoherence-free (or in this case, dephasing-free) subspace.

The work presented here significantly extends that presented by Shapiro et al. [1] by providing a way to enhance the suppression of decoherence described in that paper. In addition, the consideration of non-linear resonance induced by shaped pulse trains reveals a novel potential method of controlling vibrational wavepacket dynamics by the creation of multiple resonant "wells" of different depths along the classical trajectory. It is possible that this control method could be applied to problems other than dephasing suppression. Note that the model described above relies on certain assumptions, most notably the rotating wave approximation (see equation (3.12)). This only holds true if the fast-oscillating terms average to zero over the timescale of the rovibrational interaction. The analytical results of Chapter 2 indicate that this timescale may be as short as a few vibrational periods in typical experiments. That said, it is reasonable to assume that the dominant behaviour of the system is determined by the rotating-wave approximation, and thus the conclusions of the preceding section are sound. It is important to note laser pulse trains of the required laser frequency and pulse rate are easy to generate in the lab, and their shapes can be very precisely controlled by the use of pulse shapers, these nonlinear resonance techniques could, in principle, be tested and employed in laboratory experiments at the time of writing.

Bibliography

[1] E. A. Shapiro, I. A. Walmsley, and Misha Ivanov. Suppression of decoherence in a wave packet via nonlinear resonance. *Phys. Rev. Lett.*, 98(5):050501, 2007.

[2] H.-P. Breuer and F. Petruccione. *The Theory of Open Quantum Systems*. Oxford University Press, 2002.

[3] A. C. Doherty, A. S. Parkins, S. M. Tan, and D. F. Walls. Motional states of atoms in cavity QED. *Phys. Rev. A*, 57(6):4804–4817, Jun 1998.

[4] N. Yu, C. J. Margulis, and D. F. Coker. Influence of solvation environment on excited state avoided crossings and photodissociation dynamics. *The Journal of Physical Chemistry B*, 105(28):6728–6737, 2001.

[5] M. Wenin and W. Pötz. Minimization of environment-induced decoherence in quantum subsystems and application to solid-state-based quantum gates. *Physical Review B (Condensed Matter and Materials Physics)*, 78(16):165118, 2008.

[6] Maximilian Schlosshauer. Decoherence, the measurement problem, and interpretations of quantum mechanics. *Rev. Mod. Phys.*, 76(4):1267–1305, Feb 2005.

[7] Maximilian Schlosshauer. *Decoherence and the Quantum-to-Classical Transition*. Springer, 2007.

[8] A. G. Kofman and G. Kurizki. Unified theory of dynamically suppressed qubit decoherence in thermal baths. *Phys. Rev. Lett.*, 93(13):130406, Sep 2004.

[9] Goren Gordon and Gershon Kurizki. Universal dephasing control during quantum computation. *Phys. Rev. A*, 76(4):042310, Oct 2007.

[10] A. Galindo and M. A. Martín-Delgado. Information and computation: Classical and quantum aspects. *Rev. Mod. Phys.*, 74(2):347–423, May 2002.

[11] G. Lindblad. On the generators of quantum dynamical semigroups. *Commun. Math. Phys.*, 48(2):119–130, 1976.

[12] Sabrina Maniscalco and Francesco Petruccione. Non-markovian dynamics of a qubit. *Physical Review A (Atomic, Molecular, and Optical Physics)*, 73(1):012111, 2006.

[13] D. A. Lidar, I. L. Chuang, and K. B. Whaley. Decoherence-free subspaces for quantum computation. *Phys. Rev. Lett.*, 81(12):2594–2597, Sep 1998.

[14] Maximilian Schlosshauer, A. P. Hines, and G. J. Milburn. Decoherence and dissipation of a quantum harmonic oscillator coupled to two-level systems. *Phys. Rev. A*, 77(2):022111, 2008.

[15] E. L. Hahn. Spin echoes. *Phys. Rev.*, 80(4):580–594, Nov 1950.

[16] Paul Brumer and Moshe Shapiro. *Principles of the quantum control of molecular processes.* Wiley, 2003.

[17] P. Brumer and M. Shapiro. Coherence chemistry: Controlling chemical reactions with lasers. *Acc. Chem. Res.*, 1989.

[18] Herschel Rabitz, Regina de Vivie-Riedle, Marcus Motzkus, and Karl Kompa. Whither the Future of Controlling Quantum Phenomena? *Science*, 288(5467):824–828, 2000.

[19] Valeria D. Kleiman, Langchi Zhu, Jeanette Allen, and Robert J. Gordon. Coherent control over the photodissociation of CH_3I. *The Journal of Chemical Physics*, 103(24):10800–10803, 1995.

[20] Richard S. Judson and Herschel Rabitz. Teaching lasers to control molecules. *Phys. Rev. Lett.*, 68(10):1500–1503, Mar 1992.

[21] Robert Levis et al. Selective bond dissociation and rearrangement with optimally tailored, strong-field laser pulses. *Science*, 2001.

[22] T. C. Weinacht, J. Ahn, and P. H. Bucksbaum. Controlling the shape of a quantum wavefunction. *Nature*, 1999.

[23] Rebing Wu, Alexander Pechen, Herschel Rabitz, Michael Hsieh, and Benjamin Tsou. Control landscapes for observable preparation with open quantum systems. *J. Math. Phys.*, 2008.

[24] Ulrich Hohenester. Optimal quantum gates for semiconductor qubits. *Physical Review B (Condensed Matter and Materials Physics)*, 74(16):161307, 2006.

[25] Feng Shuang and Herschel Rabitz. Cooperating or fighting with decoherence in the optimal control of quantum dynamics. *The Journal of Chemical Physics*, 124(15):154105, 2006.

[26] M.B. Plenio and S.F. Huelga. Dephasing-assisted transport: quantum networks and biomolecules. *New J. Phys.*, 2008.

[27] Shlomo E. Sklarz, David J. Tannor, and Navin Khaneja. Optimal control of quantum dissipative dynamics: Analytic solution for cooling the three-level λ system. *Phys. Rev. A*, 69(5):053408, May 2004.

[28] John Preskill. Reliable quantum computers. *Proc. R. Soc. Lond. A*, 454(1969):385–410, January 1998.

[29] W.K. Wootters and W. H. Zurek. A single quantum cannot be cloned. *Nature*, 299:802, 1982.

[30] Peter W. Shor. Scheme for reducing decoherence in quantum computer memory. *Phys. Rev. A*, 52(4):R2493–R2496, Oct 1995.

[31] A. M. Steane. Error correcting codes in quantum theory. *Phys. Rev. Lett.*, 77(5):793–797, Jul 1996.

[32] A. R. Calderbank and Peter W. Shor. Good quantum error-correcting codes exist. *Phys. Rev. A*, 54(2):1098–1105, Aug 1996.

[33] Jan Fischer and Daniel Loss. Dealing with decoherence. *Science*, 2009.

[34] D.A. Lidar and K.B. Whaley. *Irreversible Quantum Dynamics*, pages 83–120. Springer, 2003.

[35] J. Kempe, D. Bacon, D. A. Lidar, and K. B. Whaley. Theory of decoherence-free fault-tolerant universal quantum computation. *Phys. Rev. A*, 63(4):042307, Mar 2001.

[36] Paul G. Kwiat, Andrew J. Berglund, Joseph B. Altepeter, and Andrew G. White. Experimental Verification of Decoherence-Free Subspaces. *Science*, 290(5491):498–501, 2000.

[37] D. Kielpinski, V. Meyer, M. A. Rowe, C. A. Sackett, W. M. Itano, C. Monroe, and D. J. Wineland. A Decoherence-Free Quantum Memory Using Trapped Ions. *Science*, 291(5506):1013–1015, 2001.

[38] Paolo Zanardi. Stabilizing quantum information. *Phys. Rev. A*, 63(1):012301, Dec 2000.

[39] Mark S. Byrd and Daniel A. Lidar. Comprehensive encoding and decoupling solution to problems of decoherence and design in solid-state quantum computing. *Phys. Rev. Lett.*, 89(4):047901, Jul 2002.

[40] Lorenza Viola and Seth Lloyd. Dynamical suppression of decoherence in two-state quantum systems. *Phys. Rev. A*, 58(4):2733–2744, Oct 1998.

[41] D. Vitali and P. Tombesi. Using parity kicks for decoherence control. *Phys. Rev. A*, 59(6):4178–4186, Jun 1999.

[42] Lorenza Viola, Emanuel Knill, and Seth Lloyd. Dynamical decoupling of open quantum systems. *Phys. Rev. Lett.*, 82(12):2417–2421, Mar 1999.

[43] B. Misra and E. C. G. Sudarshan. The zeno's paradox in quantum theory. *Journal of Mathematical Physics*, 18(4):756–763, 1977.

[44] Wayne M. Itano, D. J. Heinzen, J. J. Bollinger, and D. J. Wineland. Quantum zeno effect. *Phys. Rev. A*, 41(5):2295–2300, Mar 1990.

[45] A. G. Kofman and G. Kurizki. Acceleration of quantum decay processes by frequent observations. *Nature*, (405):546–550, Jun 2000.

[46] P. Facchi, D. A. Lidar, and S. Pascazio. Unification of dynamical decoupling and the quantum zeno effect. *Phys. Rev. A*, 69(3):032314, Mar 2004.

[47] Regina de Vivie-Riedle and Ulrike Troppmann. Femtosecond lasers for quantum information technology. *Chem. Rev.*, 107:5082–5100, 2007.

[48] E. A. Shapiro, Michael Spanner, and Misha Yu. Ivanov. Quantum logic approach to wave packet control. *Phys. Rev. Lett.*, 91(23):237901, Dec 2003.

[49] Kevin F. Lee, D. M. Villeneuve, P. B. Corkum, and E. A. Shapiro. Phase control of rotational wave packets and quantum information. *Phys. Rev. Lett.*, 93(23):233601, Nov 2004.

[50] Ronnie Kosloff and Stuart Rice. Comments on a semigroup formalism for the description of phase and population relaxation processes. *J. Chem. Phys*, 1980.

[51] Gil Katz, Mark A. Ratner, and Ronnie Kosloff. Decoherence control by tracking a hamiltonian reference molecule. *Phys. Rev. Lett.*, 98(20):203006, 2007.

[52] S Wallentowitz, I A Walmsley, L J Waxer, and Th Richter. Rotationally induced collapse and revivals of molecular vibrational wavepackets: model for environment-induced decoherence. *J. Phys. B*, 35(8):1967–1984, 2002.

[53] C. Brif, H. Rabitz, S. Wallentowitz, and I. A. Walmsley. Decoherence of molecular vibrational wave packets: Observable manifestations and control criteria. *Phys. Rev. A*, 63(6):063404, May 2001.

[54] J. H. Eberly, N. B. Narozhny, and J. J. Sanchez-Mondragon. Periodic spontaneous collapse and revival in a simple quantum model. *Phys. Rev. Lett.*, 44(20):1323–1326, May 1980.

[55] Matthijs P. A. Branderhorst, Pablo Londero, Piotr Wasylczyk, Constantin Brif, Robert L. Kosut, Herschel Rabitz, and Ian A. Walmsley. Coherent Control of Decoherence. *Science*, 320(5876):638–643, 2008.

[56] Bern Kohler et al. Controlling the future of matter. *Acct. Chem. Res.*, 1995.

[57] Erich Joos et al. *Decoherence and the Appearance of a Classical World in Quantum Theory.* Springer, 2003.

[58] NIST Chemistry Web-Book (http://webbook.nist.gov/).

[59] Paul Brumer and Moshe Shapiro. One photon mode selective control of reactions by rapid or shaped laser pulses: An emperor without clothes? *Chemical Physics*, 139(1):221 – 228, 1989.

[60] W. Vogel, D.G. Welsch, and S. Wallentowitz. *Quantum Optics - An Introduction.* Wiley-VCH, 2001.

[61] Gennady P. Berman, Evgeny N. Bulgakov, and Darryl D. Holm. Crossover behavior in quantum nonlinear resonance in a hydrogen atom. *Physica D: Nonlinear Phenomena*, 83(1-3):55 – 58, 1995. Quantum Complexity in Mesoscopic Systems.

[62] Benjamin J. Sussman. *Quantum Control using the Non-Resonant Stark Effect.* PhD thesis, Queen's University, Kingston, Ontario, Canada, 2006.

Control of dephasing in rotationally hot molecules

David Bartram* and Misha Ivanov

Blackett Laboratory, Imperial College London,

Prince Consort Road, South Kensington,

London SW7 2AZ, United Kingdom

(Dated: March 3, 2010)

Abstract

We consider a rotationally hot diatomic molecule as an example of an open quantum system, where molecular vibrational wavepackets are subject to dephasing due to rovibrational coupling. We report analytical and numerical results addressing whether the dephasing rate can be controlled by adjustment of the initial wavepacket phases. It appears that over long timescales, phase-only control is not possible, but for earlier timescales the possibility of phase-only control of dephasing remains. In addition, we point out that the time-dependence of the dephasing process depends significantly upon the degeneracy of the rotational environment states.

*Electronic address: david.bartram04@imperial.ac.uk

I. INTRODUCTION

An open quantum system consists of a system of interest that is coupled to an environment. Non-unitary evolution of the system can then occur, including decoherence (the reduction of the purity of the system state) which destroys coherent superpositions. Since all quantum systems in nature interact with some environment, the understanding of open system dynamics is an important topic.

In this article we consider a rotationally hot diatomic molecule, defining the system as the vibrational degree of freedom and environment as the rotational degree of freedom. This simple example of an open quantum system is relatively straightforward to examine theoretically, convenient to study experimentally, and has been actively studied [3] [4] [5]. At temperatures around 400°C (typical for production of alkali dimers from an oven source), ~ 100 rotational states J will be populated thermally. Note that the rotational state J is $(2J+1)$-fold degenerate. Since the vibrational frequency is dependent on rotational quantum number J thanks to centrifugal distortion, vibrational wavepackets moving on different (J-dependent) potential energy surfaces will dephase over time. We investigate the possibility of controlling this rotationally-induced dephasing process by shaping the initial vibrational wavepacket. The *Science* article by Branderhorst et al. [5] suggests that *phase-only* shaping of the initial wavepacket can have an effect on the dephasing rate. Our work addresses the effectiveness of such phase-only shaping in this particular system.

We report analytical and numerical results. Numerical simulations show no readily apparent effect of phase-only shaping, except by interaction between the quadratic chirp of the vibrational phases and the anharmonicity. This is just an example of the well-known wavepacket focussing [6] in an anharmonic potential, and does not relate to the thermal dephasing dynamics. In order to understand the numerical results, analytical calculations were performed, including a calculation for zero anharmonicity (the case discussed in [5]). These calculations show that over long timescales, phase-only shaping of the initial wavepacket has no effect on the dephasing. However, at intermediate timescales, the possibility of controlling the dephasing rate remains.

II. DEPHASING OF MOLECULAR VIBRATIONAL WAVEPACKETS DUE TO ROTATIONAL TEMPERATURE

A. Characterisation and measurement of wavepacket dephasing

Before discussing the details of wavepacket dynamics in a rotationally hot diatomic molecule, it is important to stress the difference between rotationally-induced dephasing and decoherence associated with entanglement between a system and its environment. This distinction is discussed, for example, in Chapter 2 of [7] and Chapter 3 of [8]. In [7] it is argued that a key distinction between classical noise or pure dephasing and real decoherence is that in the latter case, the system perturbs the environment in addition to being perturbed by it.

In the standard treatment of an open system [9], we call the Hilbert space of the system $\mathcal{H}_S$ and that of the environment $\mathcal{H}_B$, so that the Hilbert space of the total system is $\mathcal{H}_S \otimes \mathcal{H}_B$. Then the total Hamiltonian is

$$H = H_S \otimes I_B + I_S \otimes H_B + H_I \tag{1}$$

Here H_S and H_B are the free Hamiltonians of the system and environment respectively, I_S and I_B are the identity operators in the system and environment subspaces, and H_I is the interaction Hamiltonian.

We now focus on the rovibrational motion of a diatomic molecule. Within the Born-Oppenheimer approximation, assuming the molecule is in a given electronic state $|i\rangle$, it is possible [3] to re-write the rovibrational Hamiltonian for the total system in the following form.

$$\begin{aligned} H &= \frac{\hat{p}^2}{2\mu} + U_i(\hat{R}) + \frac{\hat{J}^2}{2\mu\hat{R}^2} \\ &= \left(\frac{\hat{p}^2}{2\mu} + U_i(\hat{R})\right) \otimes I_r + I_v \otimes \frac{1}{2\mu R_{eq}^2}\hat{J}^2 + \left(\frac{1}{2\mu\hat{R}^2} - \frac{1}{2\mu R_{eq}^2}\right) \otimes \hat{J}^2 \end{aligned} \tag{2}$$

Here $\hat{R}$ and $\hat{p}$ are the internuclear co-ordinate and momentum operators respectively, R_{eq} is the equilibrium internuclear distance, μ is the reduced mass, $U_i(R)$ is the molecular potential energy surface, I_r and I_v are the identity operators on the rotational and vibrational

subspaces respectively, and $\hat{J}^2$ is the angular momentum operator (in units of $\hbar^2$). In the above form, the rovibrational Hamiltonian resembles the open system Hamiltonian (1), with $H_S = \frac{\hat{p}^2}{2\mu} + U_i(\hat{R})$, $H_B = \frac{1}{2\mu R_{eq}^2}\hat{J}^2$ and $H_I = \left(\frac{1}{2\mu\hat{R}^2} - \frac{1}{2\mu R_{eq}^2}\right) \otimes \hat{J}^2$.

Note that in this case $[H_I, H_B] = 0$, so the system-environment interaction does not affect the environment states, i.e.: the rotational J-states. In this case, if the total system starts in a state $|\Psi_v(R)\rangle|J\rangle$, it evolves into $|\Psi_{v,J}(R,t)\rangle|J\rangle$, developing no entanglement. Thus, averaging over the thermal distribution in a rotational ensemble results in pure dephasing. This is to be expected, since the vibrational and rotational parts of the rovibrational wavefunction are always separable.

If the diatomic molecule is modelled as a Morse oscillator, the standard approximation for the energy of the state with vibrational quantum number v and rotational quantum number J is

$$E(v,J) = \omega_e\left(v+\frac{1}{2}\right) - \omega_e x_e\left(v+\frac{1}{2}\right)^2 + \left[B_e - \alpha_e\left(v+\frac{1}{2}\right)\right]J(J+1) - D_e J^2(J+1)^2 \quad (3)$$

Here ω_e, $\omega_e x_e$,B_e and D_e are the usual spectroscopic constants [10]. If the rotations are confined to a plane, we instead have J^2 wherever $J(J+1)$ appears in (3). Since $\langle J\rangle \approx 100 \gg 1$, this difference is negligible.

Equation (3) for $E(v,J)$ can be rewritten in the following form by introducing the J-dependent vibrational frequency $\omega_J = \omega_e - \alpha_e J(J+1)$:

$$E(v,J) = \omega_J\left(v+\frac{1}{2}\right) - \omega_e x_e\left(v+\frac{1}{2}\right)^2 + B_e J(J+1) - D_e J^2(J+1)^2 \quad (4)$$

If we have, for a molecule with a given J, a wavepacket $|\Psi_J(t)\rangle$ over the vibrational states $|vJ\rangle$ (which are J-dependent thanks to the centrifugal distortion), its time evolution is

$$|\Psi_J(t)\rangle = \sum_v a_{vJ} e^{-iE(v,J)t}|vJ\rangle \quad (5)$$

Here a_{vJ} are the wavepacket amplitudes. The rovibrational coupling term in $\omega_J = \omega_e - \alpha_e J^2$ will cause wavepackets for different J-values to dephase with each other over time [11]. This dephasing process is not irreversible; there will be revivals of the phase coherence of the ensemble. In general, however, these revivals will not coincide with the revivals due

to the anharmonicity $\omega_e x_e$, and from an observational standpoint the process looks like an irreversible dephasing.

Now we focus on the case of vibrational wavepackets created by one-photon excitation due to a laser pulse, as in the theoretical and experimental work described in references [3] and [5]. We assume that the spectral amplitudes of the pulse have their *phases* shaped at the experimenter's wish, but their *magnitudes* are unaffected by the pulse shaper. In the experiment [5] the molecules under consideration are potassium dimers at 400°C. At this temperature all molecules in the ensemble are in the electronic ground state. For simplicity, we assume that only the ground vibrational state is populated - in fact $\langle v \rangle \approx 1$ at this temperature, but the standard deviation of the thermal distribution $\Delta v_T \approx 3$, so full accuracy would require consideration of the first few vibrational levels. This assumption does not affect our conclusions since the effect of thermal occupation of different vibrational states is similar to that of rotational states. The rotational states are incoherently populated at temperature T, ie: the rotational density matrix is diagonal with populations $P(J) = Z^{-1}(2J+1)\exp\left\{\frac{-B_e J^2}{kT}\right\}$ where Z is the partition function. Here the $2J+1$ factor appears in the 3D case and is absent in the 2D case. We perform calculations both with and without this factor.

Our goal is to see whether a phase-only shaping of the wavepacket can produce substantial suppression of rovibrational dephasing. To consider control of this dephasing, it is crucial to define how the dephasing is *measured*. We follow [5] and we consider the frequency-gated fluorescence signal from the molecules. Note that this measurement is not resolved in the basis of eigenstates of the rovibrational Hamiltonian H_i - rather it is position-resolved. We can think of the contribution to the fluorescence signal from a given wavepacket $|\Psi_J(t)\rangle$ as the overlap between the wavepacket and a gate function $|\Phi_G\rangle = \sum_v g_{v,J}|vJ\rangle$. The gate is a function in space (ie: in the internuclear co-ordinate R) here given in the basis of the $|vJ\rangle$ wavefunctions. Since the form (in space) of the gate function should be exactly the same for all J, the amplitudes $g_{v,J}$ will be somewhat different for different values of J.

At this stage it is worth comparing the question posed here with the standard case of coherent control - e.g.: control of a chemical reaction. In the case where our measurement is resolved in the basis of the energy eigenstates, we can only achieve phase-only control via interference of multiple indistinguishable optical pathways [9]. Otherwise, spectral phases contribute only to phases in the various energy-eigenstate amplitudes, which have no effect

when we make a measurement in this energy eigenstate-resolved basis (since only the modulus squared of the amplitudes will affect the measured yield in each eigenstate). This is the "emperor without clothes" argument in a 1989 paper by Brumer and Shapiro [12] - an apparent avenue for control which cannot, in fact, work.

Since we do not consider multiple interfering optical pathways, it might appear that one-photon phase-only control could not possibly work for our system. But since our measurement of the dephasing is *not* resolved in the energy eigenbasis, the above argument does not apply, and phase-only control is *in principle* achievable.

The overlap between $|\Psi_J(t)\rangle$ and $|\Phi_G\rangle$ is:

$$\begin{aligned} Q(J,t) &= \langle \Phi_G | \Psi_J(t) \rangle \\ &= \sum_v g^*_{vJ} a_{vJ} e^{-iE(v,J)t} \end{aligned} \tag{6}$$

The function $Q(J,t)$ characterises the electromagnetic field emitted by a molecule in a particular J-state, and the detected signal (the intensity of the emission) is proportional to $|Q(J,t)|^2$.

$$|Q(J,t)|^2 = \sum_v \sum_{v'} A_{vJ} A_{v'J} e^{-i\left\{\omega_J(v-v') - \omega_e x_e \left[\left(v+\frac{1}{2}\right)^2 - \left(v'+\frac{1}{2}\right)^2\right]\right\}t} \tag{7}$$

Where $A_{vJ} = g^*_{vJ} a_{vJ}$ are complex numbers, and the solely J-dependent terms in $E(v,J) - E(v',J)$ have cancelled. We now assume the rovibrational coupling is weak, and neglect the J-dependence of the A_{vJ} factors. This is equivalent to neglecting the rotational distortion of the vibrational wavefunctions for the duration of the pump pulse. However for the long-term evolution, we preserve the rovibrational distortion within the J-dependent *phase*, where the effect is accumulated over time. In place of A_{vJ} we have purely v-dependent constants $A_v = |A_v| e^{i\theta_v}$.

We assume that the intensity of the laser pulse which creates our wavepacket $|\Psi_J(t)\rangle$ on an excited electronic surface is in the weak-field (perturbative) regime. This has two consequences. Firstly we may neglect the molecular alignment effect of the laser, since the aligning interaction energy will be $\ll kT$. This leaves the rotational density matrix in the form given above. Secondly, in the perturbative regime each eigenstate amplitude $|A_v| e^{i\theta_v}$ in the created wavepacket is proportional to the spectral amplitude of the laser field at the

relevant transition frequency. For this reason, phase-only shaping of the laser pulse results *solely* in adjustment of the initial phases θ_v.

Since the spontaneous emission of molecules in different J-states is not coherent, the total fluorescence signal from the thermal ensemble of molecules is proportional to:

$$S(t) = \sum_{J=0}^{\infty} P(J)|Q(J,t)|^2 \tag{8}$$

$$= \sum_{J=0}^{\infty} \sum_{v} \sum_{v'} P(J)|A_v||A_{v'}|e^{-i\left\{\theta_{v'}-\theta_v+\omega_J(v-v')-\omega_e x_e\left[\left(v+\frac{1}{2}\right)^2-\left(v'+\frac{1}{2}\right)^2\right]\right\}t} \tag{9}$$

The qualitative behaviour of these functions can be summarised as follows. As the wavepacket moves between the inner and outer turning points,$|Q(J,t)|^2$ will oscillate with the average vibrational period $\omega_{\bar{v}} = \frac{\partial E}{\partial v}|_{v=\bar{v}}$. For nonzero anharmonicity ($\omega_e x_e > 0$) the wavepacket spreads over time. $|Q(J,t)|^2$ undergoes the well-known decay and revivals - including fractional revivals - as the $E(v,J)t$ phase factors for different v's de- and re-phase with one another. In principle the J-dependent component of the phase evolution will also display revivals [4], but these will not in general coincide with the revivals due to anharmonicity. Thus the combination of anharmonic and rotational dephasing will typically result in a signal $S(t)$ which oscillates at the vibrational period, decaying over time without subsequent revival.

B. Phase-only shaping of the initial wavepacket: analytical estimates and numerical simulations

Consider the following term from equation (8)

$$E(v,J) - E(v',J) = \omega_J(v-v') - \omega_e x_e \left[\left(v+\frac{1}{2}\right)^2 - \left(v'+\frac{1}{2}\right)^2\right] \tag{10}$$

Let us introduce $k = v - \bar{v}$, where $\bar{v}$ is the average v in the wavepacket. Then

$$\begin{aligned} E(v,J) - E(v',J) &= \tilde{\omega}_J(k-k') - \omega_e x_e\left(k^2 - k'^2\right) \\ \tilde{\omega}_J &= \omega_e - 2\omega_e x_e\left(\bar{v}+\frac{1}{2}\right) - \alpha_e J^2 = \omega_{\bar{v}} - \alpha_e J^2 \end{aligned} \tag{11}$$

Here $\omega_{\bar{v}}$ is the vibrational frequency at the average v.

To approximate the signal $S(t)$ analytically, we note that we are interested in the decay of the signal, not its oscillation with vibrational frequency. We then examine the behaviour of $|Q(J,t)|^2$ at discrete time intervals $t_N = \frac{2\pi N}{\omega_{\bar{v}}}$. At times $t = t_N$ we have

$$|Q(I,t_N)|^2 = \sum_{k=-\infty}^{k=\infty} \sum_{k'=-\infty}^{k'=\infty} A_k^2 A_{k'}^2 \exp\left\{ i \left[\theta_k - \theta_{k'} + t_N \omega_e x_e (k^2 - k'^2) - t_N \Delta\Omega (k - k') I \right] \right\} \tag{12}$$

Here $\bar{J}$ is the mean rotational state, $I = J - \bar{J}$, and $\Delta\Omega = -2\alpha_e \bar{J}$.

We now assume a Gaussian amplitude profile $A_k = e^{-k^2/2\sigma^2}$ and replace the sums over discrete states with an integral over continuous variables k and k'. One effect of this approximation is to remove the possibility of revivals, but this is acceptable since we are interested in the dephasing dynamics rather than the revivals. Now consider a Taylor expansion to second order of the initial phases: $\theta_k \simeq a + bk + ck^2$. The constant term has no effect since only relative phases between levels affect the signal. A linear chirp (bk) in the laser pulse spectrum is equivalent to a translation of the pulse in the time domain. Since we are interested in the behaviour of the molecule after the pulse, we must neglect this. As a result we assume that the initial phases have only quadratic dependence in the frequency domain (ie: linear chirp in the time domain), such that $\theta_k = ck^2$.

Completing the square in the exponent and performing the necessary Gaussian integrals yields

$$|\tilde{Q}(I,t_N)|^2 \propto e^{-\kappa(t_N) I^2} |\gamma(t_N)|^{-1} \tag{13}$$

$$\gamma(t_N) = \sigma^{-2} + i(\omega_e x_e t_N + c) \tag{14}$$

$$\kappa(t_N) = \frac{1}{2} |\gamma(t_N)|^{-2} (\Delta\Omega)^2 \sigma^{-2} t_N^2 \tag{15}$$

Figure 1 shows this approximation for the case of an unchirped initial wavepacket, showing its effectiveness in representing the decay in signal due to anharmonicity.

The form of $\tilde{Q}(I,t_N)$ provides insight into the dephasing mechanism, although the true behaviour of the signal is not revealed until we average over the J-distribution. First note that the parameter $|\gamma(t_N)|^2 = \sigma^{-4} + (\omega_e x_e t_N + c)^2$ can be viewed as a measure of wavepacket

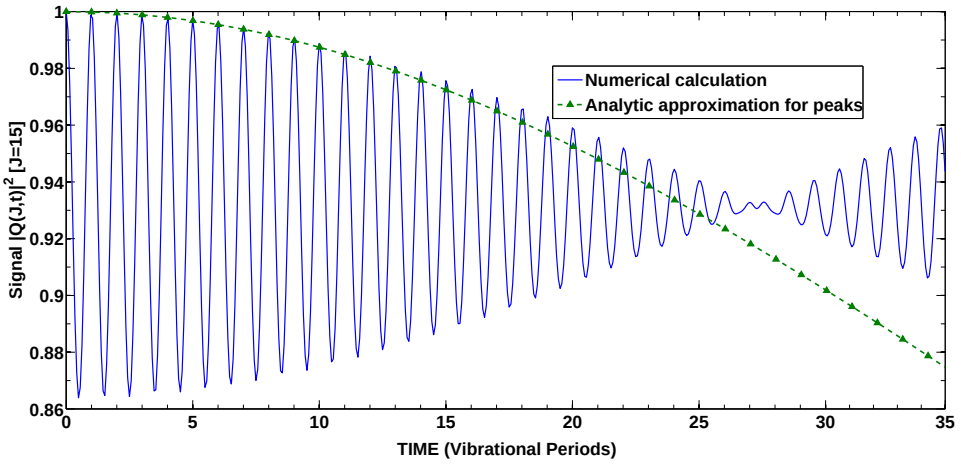


FIG. 1: (Color online) For the case of flat initial phases ($\theta_v = 0 \forall v$), the J=15 contribution to the signal $\frac{|Q(15,t)|^2}{max[|Q(15,t)|^2]}$ (solid blue line) is compared to the analytic approximation for the peaks $\tilde{Q}(J, NT)$ (dashed green line), where T is the vibrational period and N is an integer. The decay and revival of the single-J contribution seen here is due to the anharmonicity. The figure shows that while the approximation fails to capture the revival dynamics, it approximates the decay quite closely.

broadness in space. The σ^{-4} term captures the fact that a wavepacket in which few energy levels participate is broad in position space, while the $(\omega_e x_e t_N + c)^2$ term shows the anharmonic broadening and the effect of the chirp. Notice that $\gamma(0)$ is increased by either a positive or negative chirp: chirping the phases broadens the initial wavepacket. We also so see that for a negative chirp, the anharmonicity will first *narrow* the wavepacket before broadening it. The wavepacket will be at its most narrow when $t_N = \frac{c}{\omega_e x_e}$.

In equation (13) we see that the broadness parameter $|\gamma(t_N)|^2$ appears both in the outer factor and within the exponential. The outer factor ensures that at any given time, a broader wavepacket will give a lower signal than a narrower one, since it will have a reduced overlap with the localised gate function. The role of $|\gamma(t_N)|^{-2}$ in the exponent is to decrease the instantaneous rate of decay of the signal for broader wavepackets. It may appear surprising that such decay occurs in $|\tilde{Q}(I, t_N)|^2$, because for a single rotational state $I = J - \bar{J}$ there is no dephasing. Recall that the times t_N are multiples of the *mean* vibrational period. For nonzero I, this is not the period that the wavepacket will actually move with. The decay in $|\tilde{Q}(I, t_N)|^2$ is due to this disparity.

For a given value of I, the signal for a broader wavepacket will decay more slowly over time. This can be understood by considering the extreme cases - a narrow δ-function-like peak (call this wavepacket $\Psi_N(R,t)$) and a broad wavepacket that is completely spread out along the classical trajectory (call this $\Psi_B(R,t)$). $\Psi_B(R,t)$ does not move along the trajectory as time increases, so its overlap with the gate function $\Psi_G(R)$ is small but constant. $\Psi_N(R,t)$ on the other hand, gives a strong signal when it is located on top of the gate function but if it is located away from the gate function then its overlap will vanish. So even a minor disparity between the wavepacket's period and the mean vibrational period will cause the signal for $\Psi_N(R,t)$ to decay rapidly.

Now we turn to the averaging over the J-distribution. Let $\beta = B_e/kT$. Substituting into equation (8) and again replacing the sum with an integral, we have

$$\tilde{S}(t_N) \propto |\gamma(t_N)|^{-1} \int_0^\infty dJ e^{-\beta J^2 - \kappa(t_N)(J-\bar{J})^2} \tag{16}$$

By completing the square in the exponent, we can rewrite this as follows:

$$\tilde{S}(t_N) \propto |\gamma(t_N)|^{-1} e^{-\kappa(t_N)\bar{J}(\bar{J}-J')} \int_0^\infty dJ e^{-(\beta+\kappa(t_N))(J-J')^2} \tag{17}$$

$$J' = \frac{\kappa(t_N)\bar{J}}{\beta + \kappa(t_N)} \tag{18}$$

The solution to the integral is expressed in terms of the complementary error function

$$\mathrm{erfc}(x) \propto \int_x^\infty dy e^{-y^2}$$

as

$$\tilde{S}(t_N) \propto |\gamma(t_N)|^{-1} e^{-\kappa(t_N)\bar{J}(\bar{J}-J')(\beta+\kappa(t_N))^{-\frac{1}{2}}} \mathrm{erfc}(-(\beta+\kappa(t_N))^{\frac{1}{2}} J') \tag{19}$$

Fig. 2 shows this analytic approximation, compared to the full $S(t)$ calculated numerically. Fig. 3 shows the result when the initial phases have a quadratic chirp $c = -0.1$.

The key result here is that in this model, contrary to the claim of Branderhorst et al. [5], negatively chirping the initial phases does not produce a wavepacket that is inherently

resistant to the rovibrational dephasing. Instead we see that this produces an initially broadened wavepacket which is narrowed due to the anharmonicity, so that the signal first improves over time and subsequently decays. If there is no anharmonicity, this effect is not present.

We can study this effect qualitatively if we take the lower limit of the integral in equation (17) to $-\infty$. This approximation is justified since the factor $e^{-\kappa(t_N)J'^2}$ is small and goes quickly to zero as t_N increases. This yields

$$\tilde{S}_{-\infty}(t_N) = [(t_N - t')A + B]^{-\frac{1}{2}} \tag{20}$$

$$A = \beta(\omega_e x_e)^2 + \sigma^{-2}(\Delta\Omega)^2 \tag{21}$$

$$B = \beta(\sigma^{-4} + c^2) - At'^2 \tag{22}$$

$$t' = \frac{-\beta c\omega_e x_e}{A} \tag{23}$$

Since $t' \propto -c$, we can see the origin of the time-translation of the signal peak when a chirp is introduced. If we neglect the $\sigma^{-2}(\Delta\Omega)^2$ term in A, $t' = \frac{-c}{\omega_e x_e}$, which is the time at which the signal for a single value of I (or equivalently J) has its maximum, see equation (13). While this approximation to the signal is less accurate than equation (17), its behaviour is easier to understand. In this approximation the introduction of chirped initial phases simply time-shifts the entire signal. The behaviour of the numerically calculated $S(t)$ and the approximations $\tilde{S}(t_N)$ and $\tilde{S}_{-\infty}(t_N)$ are all qualitatively consistent. In this model, there is no sign of quadratically chirped phases providing any increase in inherent resistance to "decoherence", contrary to [5].

C. Phase- and amplitude-shaping: squeezed coherent wavepacket and two-state wavepacket

Branderhorst et al. [5] argue that initially position-squeezed wavepackets are more resistant to dephasing, since position-squeezed wavepackets are approximate eigenstates of the interaction Hamiltonian [3]. Although such a wavepacket is not position-squeezed at all times, it spends most of its time near the classical turning points, where it is position-squeezed. This section addresses whether this resistance to dephasing is observed in our

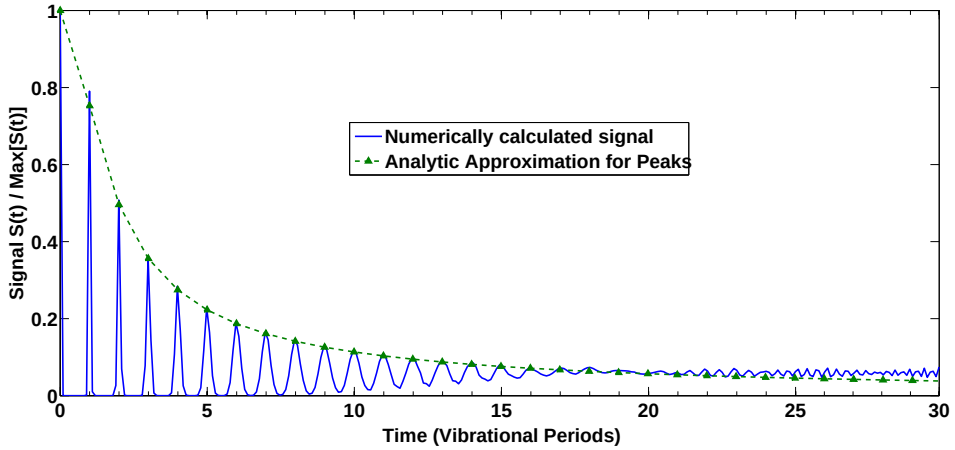


FIG. 2: (Color online) For the case of flat initial phases ($\theta_v = 0 \forall v$), the normalised signal function $\frac{S(t)}{max[S(t)]}$ (solid blue line) is compared to the analytic approximation for the peaks $\tilde{S}(NT)$ (dashed green line), where T is the vibrational period and N is an integer. The analytic approximation shows good qualitative agreement with the numerical results, demonstrating that the analytic approximation captures the decay of the signal due to rovibrational coupling.

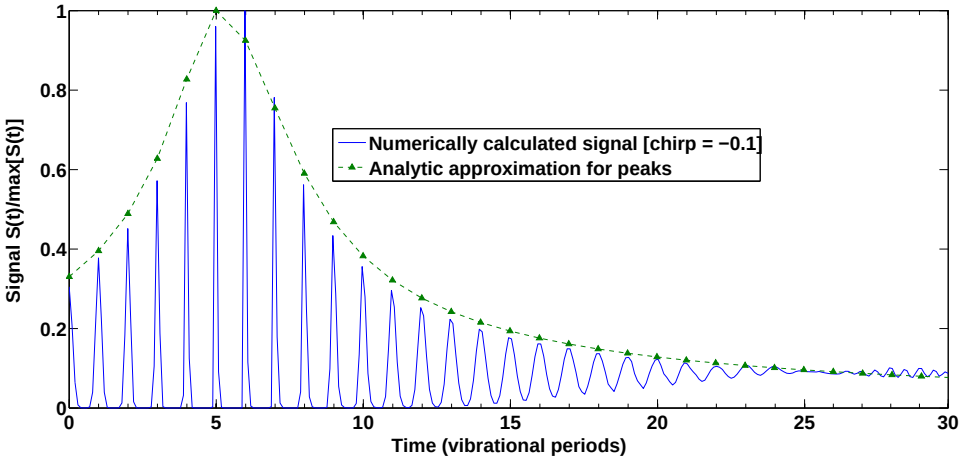


FIG. 3: (Color online) The same as Fig. 2, but with a negative quadratic chirp to the initial phases ($\theta_v = -0.1(v - \bar{v})^2$). Again there is good qualitative agreement - the analytic model shows a similar rise and fall.

model. In order to test this, we set the anharmonicity equal to zero and choose the initial vibrational wavepacket to be a squeezed coherent wavepacket displaced to the inner turning point. Creating such a wavepacket would require substantial amplitude- and phase-

modulation of the excitation pulse.

The complex amplitudes of each harmonic oscillator eigenstate in a squeezed coherent wavepacket $|\beta_c, \xi\rangle$ with displacement parameter β_c and squeezing parameter $\xi = |\xi| e^{i\phi_\xi}$, may be written in the form below [13], where $\mu = \cosh|\xi|$ and $\nu = e^{i\phi_\xi} \sinh|\xi|$. When the displacement $\beta_c = \pi$ and the squeezing factor ξ is real, we have the desired radially-squeezed wavepacket at the inner turning point (we take $\xi = 0.8$).

$$A_n^c e^{i\theta_n^c} = \left(\frac{\nu}{2\mu}\right)^{\frac{n}{2}} \frac{1}{\sqrt{\mu n!}} \exp\left[-\frac{1}{2}\left(|\beta_c|^2 - \frac{\nu^*}{\mu}\beta_c^2\right)\right] H_n\left(\frac{\beta_c}{\sqrt{2\mu\nu}}\right) \tag{24}$$

We also consider the wavepacket $|\Psi_2\rangle = \frac{1}{\sqrt{2}}(|\bar{v}\rangle + |\bar{v}+1\rangle)$ containing only two adjacent vibrational levels, which will also show beating at vibrational frequency. Figure 4 shows the signals calculated for the wavepacket with Gaussian amplitude profile and the squeezed coherent wavepacket. At a first glance, it appears that there is substantial difference in the surrogate measure of decoherence expressed by $S(t)$, for the three initial wavepackets. However, this first impression is incorrect. In order to assess their dephasing rate, the extrema of these curves are extracted and used to calculate a visibility $V = \frac{S_{\text{peak}} - S_{\text{valley}}}{S_{\text{peak}} + S_{\text{valley}}}$ for each period. This visibility is plotted as a function of time in Figure 5. Surprisingly, the three curves are nearly identical, showing no resistance to the dephasing process for the squeezed wavepacket $|\beta_c, \xi\rangle$ or the two-state wavepacket $|\Psi_2\rangle$.

The analytic work in the following sections is motivated by the need to explain why such drastic amplitude- and phase-adjustments of the initial wavepacket seem to have no effect on the dephasing process, contrary to the conclusions of [3] and [5].

D. Analytical investigation of the signal function $S(t)$

Since we are interested solely in the dephasing due to thermal rotational population, for the following calculation we will neglect the anharmonicity $\omega_e x_e$. In contrast to the previous calculation, where we have looked at $S(t)$ at specific moments, here we will look at the complete time-dependence. The main approximation is to replace the summation over J with an integral. We perform the integral before the summation over v and v'. To simplify the J-integral, we shall assume that the bath distribution is $P(J) \propto 2Je^{\frac{-BJ^2}{kT}}$. We will also probe the dependence of $S(t)$ on the distribution of bath states by comparing the result for

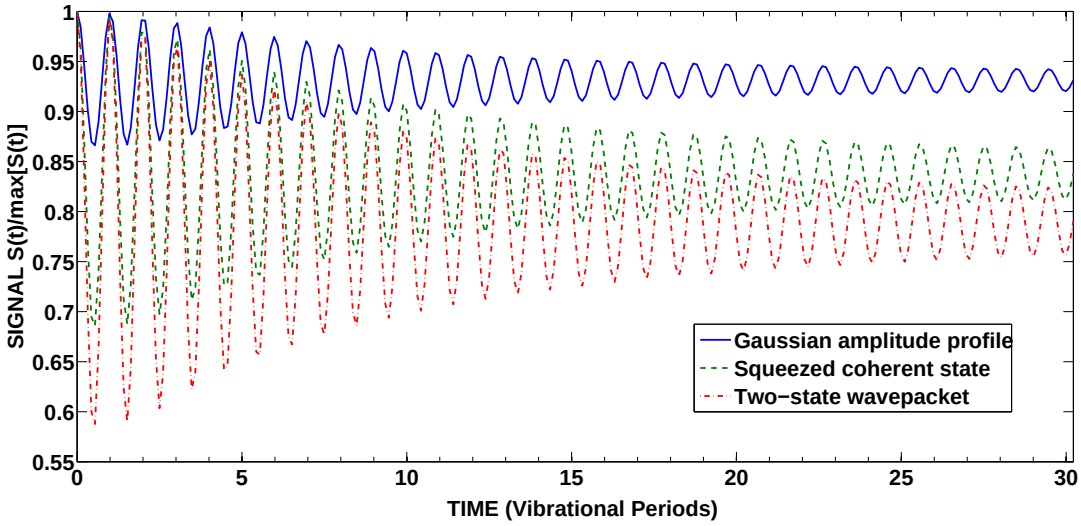


FIG. 4: (Color online) The normalised signals as a function of time for three different initial vibrational wavepackets. The first has a Gaussian amplitude profile $|\Psi_g\rangle = \sum_k e^{-k^2/2\sigma^2}|k\rangle$ (solid blue line), the second is a position-squeezed coherent wavepacket at the inner turning point $|\beta_c = \pi, \xi = 0.8\rangle$ (dashed green line) and the third is the wavepacket consisting of two adjacent vibrational states $|\Psi_2\rangle = \frac{1}{\sqrt{2}}(|\bar{v}\rangle + |\bar{v}+1\rangle)$ (dot-dashed red line). Here anharmonicity is zero, so the decay in the signal visibility is purely due to the rovibrational coupling.

$P(J) \propto 2Je^{\frac{-BJ^2}{kT}}$ with that for the 2-D distribution $P_{2D}(J) \propto e^{\frac{-BJ^2}{kT}}$. The true 3-D thermal distribution, then, is proportional to the sum of these two distributions.

Performing the J-integral yields

$$S(t) \propto \sum_v \sum_{v'} A_v A_{v'} e^{-i\omega_e(v-v')t} \frac{1 + i\alpha_e J_0^2 (v-v')t}{1 + \alpha_e^2 J_0^4 (v-v')^2 t^2} \tag{25}$$

Here $J_0^2 = kT/B_e$. Now we define time-dependent phases $\Phi_{vv'} = \omega_e(v-v')t - (\theta_v - \theta_{v'})$ (determined by the pure vibrational dynamics) and $\phi^{\alpha}_{vv'} = \arctan\left(\alpha_e J_0^2 (v-v')t\right)$ (determined by the dynamics due to rovibrational coupling). Then we may use the fact that $S(t)$ is real to write equation (25) in the following form:

$$S(t) \propto \sum_v \sum_{v'} |A_v||A_{v'}| \frac{1}{\sqrt{1 + \alpha_e^2 J_0^4 (v-v')^2 t^2}} \cos\left(\Phi_{vv'} - \phi^{\alpha}_{vv'}\right) \tag{26}$$

A first glance at equation (26) might suggest that the rovibrational coupling has little

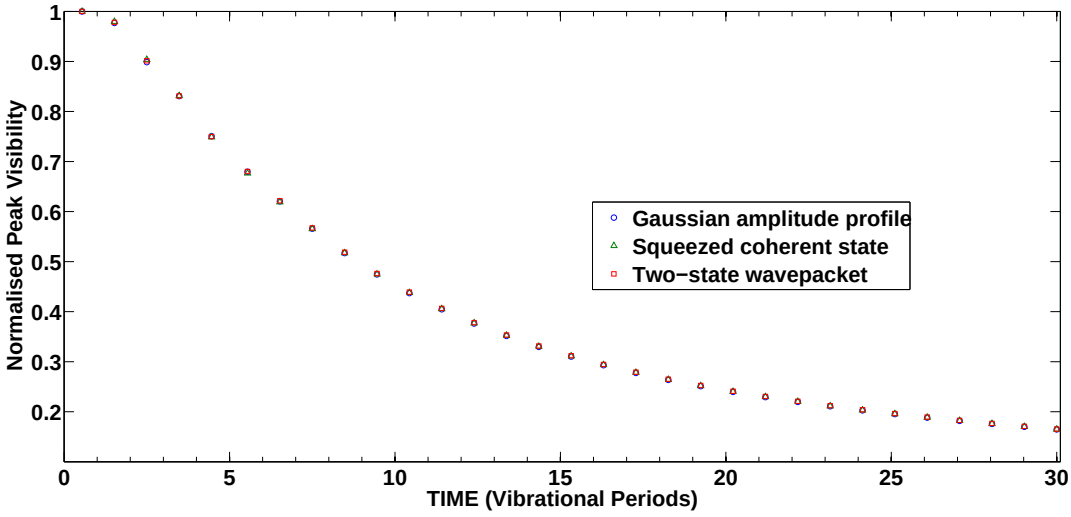


FIG. 5: (Color online) The normalised peak visibility $V/\max[V]$ as a function of time (extracted from Figure 4) for the three initial wavepackets $|\Psi_g\rangle$ (blue circles),$|\beta_c = \pi, \xi = 0.8\rangle$ (green triangles) and $|\Psi_2\rangle$ (red squares). This shows that for our model, these three different wavepackets show the same dephasing behaviour over time.

effect. The coherences between the levels with different $v \neq v'$ decrease as $\frac{1}{t}$ at long times and quadratically at short times. However, it is important to look closely at the effect of $\phi^{\alpha}_{vv'} = \arctan\left(\alpha_e J_0^2 (v - v')t\right)$.

Let Δv be the characteristic full width of the wavepacket in v. In addition, assume $\Delta v \gg 1$. Then we can separate three main timescales.

1) Short timescales $\Delta v \alpha_e J_0^2 t \ll 1$: In this case we have $\phi^{\alpha}_{vv'} \simeq \alpha_e J_0^2 (v - v')t$. Then, $\alpha_e J_0^2$ merely acts as a correction to the vibrational frequency ω_e, otherwise leaving the vibrational dynamics undisturbed:

$$S(t) \propto \sum_v \sum_{v'} |A_v||A_{v'}| \frac{1}{\sqrt{1 + \alpha_e^2 J_0^4 (v - v')^2 t^2}} \cos\left[\omega_{J_0}(v - v')t - (\theta_v - \theta_{v'})\right] \tag{27}$$

Here $\omega_{J_0} = \omega_e - \alpha_e J_0^2$ is the rotationally-adjusted vibrational frequency. Maxima in $S(t)$ occur at times $t_n = \frac{2\pi n}{\omega_{J_0}}$.

2) Long timescales $\Delta v \alpha_e J_0^2 t \gg 1$: For this case, $\phi^{\alpha}_{vv'} \simeq \frac{\pi}{2}\text{sign}(v - v')$ becomes inde-

pendent of v and the signal is given by

$$S(t) \propto S_0 + 2\sum_v \sum_{v'<v} |A_v A_{v'}| \frac{1}{\alpha_e J_0^2 |v-v'| t} \sin \Phi_{vv'} \tag{28}$$

Here $S_0 = \sum_v |A_v|^2$. Note that $\cos(\Phi_{vv'} - \phi^\alpha_{vv'})$ has been replaced with $\sin \Phi_{vv'}$, meaning that the maxima have shifted by $\frac{\pi}{2}$ compared to the very early times. The height of the maxima (thus also the contrast) is decreasing with time as $\frac{1}{t}$. Initial adjustments of θ_v can have *no* effect on the dephasing in this long-time limit, since the rovibrational coupling has disappeared from the phases completely. It remains only in the slowly decreasing envelope.

3) Intermediate timescales $\Delta v \alpha_e J_0^2 t \gtrsim 1$: $\phi^\alpha_{vv'}$ depends upon $v - v'$. Namely, for $v - v' = 1, 2$ we have $\phi^\alpha_{vv'} \lesssim 1$ and the maxima are at positions $t_n = \frac{2\pi n}{\omega_{J_0}}$. But for distant parts of the wavepacket, where $v - v'$ is large, we have a different situation, and $\phi^\alpha_{vv'} \simeq \frac{\pi}{2}$. So for different parts of the wavepacket, their contributions to $S(t)$ reach their maxima and minima at different times, and this reduces the overall contrast when we sum over v and v'. One can in principle compensate for this spread of maxima and minima with the initial phases θ_v. However, we will not be able to do so with a linear or quadratic chirp, since $\phi^\alpha_{vv'}$ is a non-linear function of $v - v'$.

E. Explanation for the Numerical Results of Section II C

At this stage we may reconsider the numerical results of Section II C, in particular Figure 5. Although the analytic results above do not address the visibility directly, we can ask whether they provide any qualitative explanation for the fact that the decay of visibility is the same for the three wavepackets (wavepacket with Gaussian amplitude profile $|\Psi_g\rangle$, the squeezed coherent wavepacket $|\beta_c, \xi\rangle$, and the wavepacket containing only two adjacent states $|\Psi_2\rangle$). It is clear from examining equation (28) that the long-term behaviour of the wavepacket will be unaffected by the initial phases, and dominated by the terms in the sum where $v - v'$ is small. So for both $|\Psi_g\rangle$ and $|\beta_c, \xi\rangle$ the dominant dynamics is the beating between the mean $\bar{v}$ and adjacent states - the contribution from nearest-neighbour pairs away from the mean is suppressed due to the decay of the amplitudes A_v away from their maximum $A_{\bar{v}}$. At long timescales the behaviour of both of these wavepackets will be very similar to

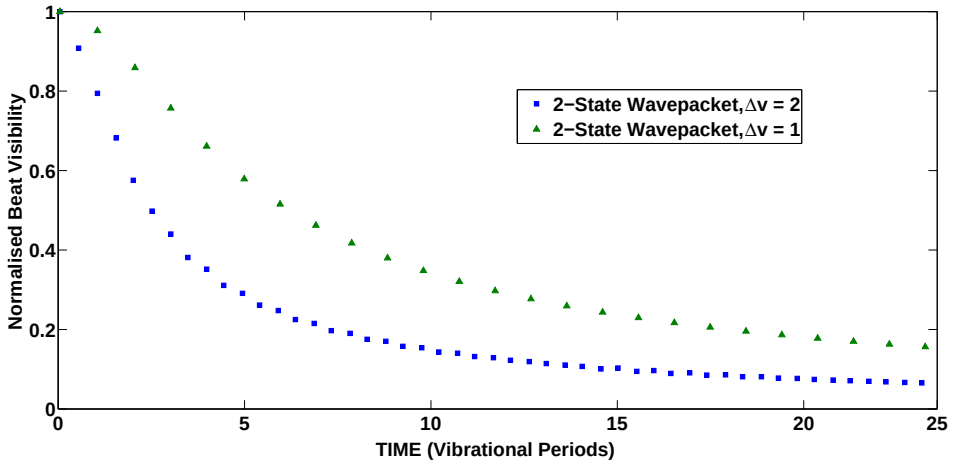


FIG. 6: (Color online) The normalised peak visibility $V/\max[V]$ as a function of time for two initial wavepackets, each containing only two vibrational states separated by Δv. Naturally, the case where $\Delta v = 2$ ($|\chi_2\rangle$) (blue squares) beats with twice the frequency of $\Delta v = 1$ ($|\Psi_2\rangle$) (green triangles) . We see that the dephasing behaviour over time is different for the two wavepackets, with the $\Delta v = 2$ wavepacket dephasing more rapidly than the wavepacket with $\Delta v = 1$. This demonstrates a case where *amplitude* modulation of the initial wavepacket has a significant effect on the dephasing dynamics.

that of $|\Psi_2\rangle$. Note that for the parameter values used in the numerical simulation, which reflect the typical J_0^2 value in an experimental setup, the long-timescale limit $\Delta v \alpha_e J_0^2 t \gg 1$ is achieved after only a few vibrational periods. This provides a qualitative explanation for the form of Figure 5. Equation (28) also shows that while these three wavepackets behave similarly, the dephasing is not completely unaffected by amplitude modulation of the initial wavepacket. As an example we took another two-state wavepacket $|\chi_2\rangle = \frac{1}{\sqrt{2}}\left(|\bar{v}\rangle + |\bar{v}+2\rangle\right)$ and compared its dephasing to $|\Psi_2\rangle$in Figure 6. We see that this *amplitude* modulation has a substantial effect on the dephasing rate.

F. Dependence on the Bath Distribution

One question that is worth considering when looking at a model of environment-induced dephasing, is the following: how sensitively does the dephasing dynamics depend upon the exact distribution of population among the environment states? In order to address this

question in our model, we repeat the calculation of Section II D using the 2-D rotational bath distribution $P_{2D}(J) \propto e^{\frac{-BJ^2}{kT}}$. Substituting this into equation (8) and approximating the sum as an integral as in (25), yields the following result (c.f. equation 26)

$$S(t) \propto \sum_{v} \sum_{v'} |A_v A_{v'}| (1 + \alpha_e^2 J_0^4 (v - v')^2 t^2)^{-\frac{1}{4}} \cos\left(\Phi_{vv'} - \tilde{\phi}_{vv'}\right) \tag{29}$$

Where $\tilde{\phi}_{vv'} = -\frac{1}{2}\phi^{\alpha}_{vv'}$ and all other quantities are defined as in Section II D above. Therefore, changing the bath distribution alters the ro-vibrational dephasing angle from $\phi^{\alpha}_{vv'}$ to $\tilde{\phi}_{vv'}$ and changes the signal decay with time, so that at long times instead of decay $\propto \frac{1}{t}$ we have $\propto \frac{1}{\sqrt{t}}$. These changes - particularly the latter - are substantial. This result shows that here we have a very strong dependence of our outcome on the details of the environment states - namely the degeneracy of each J-level.

III. CONCLUSIONS

In this paper we have studied rotationally-induced dephasing of vibrational wavepackets in hot diatomic molecules, with a view to establishing whether phase-only adjustments of the initial wavepacket can affect the rate of dephasing. An analytical investigation of the fluorescence signal $S(t)$ determined that there are three relevant timescales, determined by the size of the parameter $\Delta v \alpha_e J_0^2 t$. At short timescales, dephasing has not set in and there is no need to compensate for it. At long timescales, which can be reached after as little as a few vibrational periods in typical experiments, the dephasing process can no longer be compensated at all by initial wavepacket phases. Between these limits, there is an intermediate timescale where adjustments of the initial phases can, in principle, affect the dephasing rate.

The form for the signal $S(t)$ in equation (26) makes it clear that phase-only control of the dephasing means compensating for $\phi^{\alpha}((k-k'),t) = \arctan\left(\alpha_e J_0^2 (k-k')t\right)$ by selecting the values of the initial phases θ_k, where $k = v - \bar{v}$. At intermediate times we may no longer treat the arctan in ϕ^{α} as linear. Expanding it to third order we get $\phi^{\alpha}_{kk'} \simeq \alpha_e J_0^2 (k-k')t - \frac{1}{3}\alpha_e^3 J_0^6 (k-k')^3 t^3$, so we would need a cubic term in the phases to compensate for this. In our numerical simulations we have tried various values of cubic chirp in the initial phases, but none have reduced the dephasing rate. To explain the difficulties with phase-only control of

the dephasing, let us assume that the initial phases are $\theta_k = bk + ck^2 + dk^3$. Then the phase $\Theta(k, k', t) = \Phi_{kk'} - \phi^{\alpha}_{kk'}$ in equation (26) can be written as follows (letting $n = k - k'$ and $m = k + k'$)

$$\begin{aligned} \Theta(n, m, t) &= F_0(n) + F_1(n)m + F_2(n)m^2 \\ F_0(n) &= \omega_e n - bn - \phi^{\alpha}(n, t) + \frac{1}{4}dn^3 \\ F_1(n) &= -cn \\ F_2(n) &= -\frac{3}{4}dn \end{aligned} \tag{30}$$

Now we assume that the constants A_k are Gaussian, i.e. $|A_k| = e^{-\frac{k^2}{k_0^2}}$. Then equation (26) gives

$$S(t) \propto \sum_n \sum_m \frac{e^{-\frac{n^2}{2k_0^2}}}{\sqrt{1 + \alpha_e^2 J_0^4 t^2 n^2}} e^{-\frac{m^2}{2k_0^2}} \cos\left[F_0(n) + F_1(n)m + F_2(n)m^2\right] \tag{31}$$

The first thing to note is that the initial phases, which appear only inside the cosine, cannot affect the term $(1 + \alpha_e^2 J_0^4 t^2 n^2)^{-\frac{1}{2}}$. So there is some overall decay in the signal which cannot be avoided by adjusting the initial phases. Secondly, examination of F_0 shows that the cubic chirp d can compensate for the rotational phase ϕ^{α}. However, the cubic chirp d *also* appears in F_2 - so when we perform the double sum over n and m, this introduces a further phase scrambling in addition to the thermal dephasing. It is clear from our analysis that phase-only suppression of the dephasing process is a challenging proposition, and even when it is achieved, it can only operate over a limited timescale.

The question remains as to why our conclusions differ substantially from those of Branderhorst et al. [5], who reported control of the dephasing process by application of quadratically-chirped excitation pulses. The key assumption in our model is neglecting the effect of rotational distortion of the vibrational wavefunctions during the pump pulse, i.e. neglecting the J-dependence of the A_{vJ} factors in equation (7). It is possible that phase-only control is more easily achieved if these distortions are taken into account.

---

[1] A. Galindo and M. A. Martín-Delgado, Rev. Mod. Phys. **74**, 347 (2002).

[2] A. G. Kofman and G. Kurizki, Phys. Rev. Lett. **93**, 130406 (2004).

[3] C. Brif, H. Rabitz, S. Wallentowitz, and I. A. Walmsley, Phys. Rev. A **63**, 063404 (2001).

[4] S. Wallentowitz, I. A. Walmsley, L. J. Waxer, and T. Richter, J. Phys. B **35**, 1967 (2002), URL `http://stacks.iop.org/0953-4075/35/1967`.

[5] M. P. A. Branderhorst, P. Londero, P. Wasylczyk, C. Brif, R. L. Kosut, H. Rabitz, and I. A. Walmsley, Science **320**, 638 (2008), http://www.sciencemag.org/cgi/reprint/320/5876/638.pdf, URL `http://www.sciencemag.org/cgi/content/abstract/320/5876/638`.

[6] B. Kohler et al., Acct. Chem. Res. (1995).

[7] M. Schlosshauer, *Decoherence and the Quantum-to-Classical Transition* (Springer, 2007).

[8] E. Joos et al., *Decoherence and the Appearance of a Classical World in Quantum Theory* (Springer, 2003).

[9] H.-P. Breuer and F. Petruccione, *The Theory of Open Quantum Systems* (Oxford University Press, 2002).

[10] *NIST Chemistry Web-Book (http://webbook.nist.gov/).*

[11] J. H. Eberly, N. B. Narozhny, and J. J. Sanchez-Mondragon, Phys. Rev. Lett. **44**, 1323 (1980).

[12] P. Brumer and M. Shapiro, Chemical Physics **139**, 221 (1989), ISSN 0301-0104, URL `http://www.sciencedirect.com/science/article/B6TFM-44GH8D7-NH/2/fca7a12a92254126dcc5f6ba42c6bc36`.

[13] W. Vogel, D. Welsch, and S. Wallentowitz, *Quantum Optics - An Introduction* (Wiley-VCH, 2001).